Mechanical Performance of Foam-Infilled 3D-Printed Corrugated Core Sandwich Panels: Experimental and Numerical

Marjan Abdali

A Thesis in
The Department of
Mechanical, Industrial, and Aerospace Engineering

Presented in Partial Fulfillment of the
Requirements for the Degree of Master of
Applied Science (Mechanical Engineering) at
Concordia University
Montreal, Quebec, Canada

February 2025

CONCORDIA UNIVERSITY

School of Graduate Studies

This is to certify that the thesis prepared

By: Marjan Abdali

Entitled: Mechanical Performance of Foam-Infilled 3D-Printed Corrugated Core Sandwich Panels: Experimental and Numerical

and submitted in partial fulfillment of the requirements for the degree of

Master of Applied Science (Mechanical Engineering)

complies with the regulations of the University and meets the accepted standards with respect to originality and quality.
Signed by the final Examining Committee:

______________________________ Chair

Dr. Suong Van Hoa

______________________________ Examiner

Dr. Suong Van Hoa

______________________________ Examiner

Dr. Farah Hafeez

______________________________ Supervisor

Dr. Mehdi Hojjati

Approved by ____

Dr. Muthukumaran Packirisamy

Chair of the Department of Mechanical, Industrial, and Aerospace Engineering

February 25, 2025 ____

Date Dr. Mourad Debbabi

Dean, Faculty of Engineering and Computer Science

ABSTRACT

Mechanical Performance of Foam-Infilled 3D-Printed Corrugated Core Sandwich Panels: Experimental and Numerical

Marjan Abdali

This study investigates the mechanical performance of 3D-printed corrugated core sandwich panels under compression and bending loads through experimental and numerical methods. Initially, panels were fabricated with polylactic acid (PLA) skins and cores featuring triangular, trapezoidal, rectangular, and circular geometries. Experimental testing revealed that rectangular cores exhibited the highest compression strength, while triangular cores performed best under bending due to their superior stiffness-to-weight ratio. The circular and trapezoidal cores were found to maintain median performance under both compression and bending. Various failure mechanisms were observed within the corrugated core samples, including buckling, delamination, and core fracture. Subsequently, recycled polyethylene terephthalate (PET) foam inserts were added to the corrugated core channels to further improve the performance of the panel. The foam, recognized for its high strength-to-weight ratio, moisture resistance, and thermal insulation properties, significantly increased the compressive strength of the panels by 200-345% with only a 32.5% increase in weight. Similarly, the flexural strength improved by 170-267% while the weight increased by an average of 40%. The foam inserts delayed buckling, improved structural stability, and enhanced the ability of the panels to absorb energy under load. With the addition of foam failure, mechanisms such as foam fracture, densification, and foam shear were observed. Ultimately, finite element models were developed on ABAQUS for each core geometry. These models enabled the simulation of both compression and bending performance, evaluating the effect of change in geometric parameters and optimizing corrugated core structures. The model's predictions were validated against experimental results, showing good correlation and providing insight into how different geometries influence mechanical behavior. The simulation helps identify optimal designs for enhanced load-bearing capacity and energy absorption by adjusting core geometry. These results emphasize the importance of core geometry and foam inserts in optimizing sandwich panel designs for multi-functional and high-performance applications within diverse industries.

ACKNOWLEDGMENTS

I would like to express my appreciation to my supervisor, Dr. Mehdi Hojjati, for his invaluable guidance, constructive feedback, and unwavering support throughout my research. His expertise and trust in my work have been instrumental in shaping my thesis.

I would also like to extend my gratitude to ICP Inc. for their collaboration and support. A special thanks to Mr. Moghaddar for his insightful feedback and assistance, which have contributed to the direction and quality of my work.

I appreciate the Concordia community fostering a collaborative and supportive environment. I would also like to acknowledge Nazanin, Parinaz, Sepanta, Ehsan, Meisam, Hafez, Farshad, and Arsalan for their support and camaraderie throughout this journey.

Finally, I extend my deepest gratitude to my family. Their unwavering encouragement, patience, and support have been fundamental to my perseverance and success.

Table of Contents

LIST OF FIGURES

LIST OF TABLES

Chapter 1: INTRODUCTION

1.1 Background

It is widely known that sandwich panels are universally utilized across various industries due to their high strength and stiffness-to-weight ratio. They play a vital role in many industries, such as aerospace, marine, automotive, and construction. Composite sandwich structures typically have two face sheets and a central lightweight core. The face sheets provide most of the stiffness and strength, while the addition of a core in the middle of the laminate improves the flexural stiffness of the material. Sandwich panels have high bending resistance, stiffness, and shock absorption capability. The performance of sandwich structures is primarily influenced by the topological design of the core and the selection of the material [1,2]. Over the years, materials used as the core of sandwich panels range from balsa wood and metals to foams and advanced composites [3-5]. Composites have been a trending material for sandwich panels due to their superior mechanical properties, lightweight, corrosion and chemical resistance. However, their relatively high cost and complex manufacturing process make other materials, such as metals, a more effective choice due to their structural rigidity, cost-effectiveness, and ease of fabrication. Each of the core materials has its specific advantages and disadvantages; the choice of core material will depend on the specific requirements of the application, including weight, strength, cost, and ease of fabrication [6,7].

As previously stated, one of the significant factors affecting the performance of sandwich panels is the core geometry. Conventional core geometries utilized in sandwich panels include honeycomb, truss cores, and corrugated cores [8]. Similar to the selection of materials, each geometry is intended for a particular application. Corrugated core sandwich panels offer excellent mechanical properties, excellent energy absorption capabilities, address moisture retention issues, and are easier to manufacture compared to honeycomb core panels [9,10]. In contrast to honeycomb cores, a corrugated core opposes bending and twisting as well as vertical shear [11]. The design of the corrugated core results in a superior structure that can absorb and distribute energy from impact, making it more resistant to damage and can increase the overall stiffness of the structure [12].

Honeycomb and foam core sandwich panels have the potential to absorb and lock in the moisture within the structure, which can lead to an increase in the weight and degrade the properties of the core. Open channel cores have been suggested by multiple researchers to prevent issues related to moisture retention as they provide outstanding ventilation characteristics [13]. The difficulty of manufacturing a corrugated core depends on the material and the geometry of the core, but they are more tolerant to manufacturing errors and variations, which can lead to more consistent and reliable performance of the final product [11]. Due to these reasons, corrugated core sandwich panels are progressively used in the aerospace, construction, marine, and transport industries. The challenge experienced with selecting corrugated core sandwich panels is the wide variety of available geometries. Each of these unique geometries presents opportunities and challenges in terms of mechanical performance, manufacturing complexity, and weight. As a result, many studies have been conducted comparing different core geometries under different types of mechanical loading.

One of the challenges of studies where multiple core geometries are investigated is sample manufacturing. In order to compare and optimize different corrugated geometries, a rapid prototyping method is required. Manufacturing each sample geometry using traditional processes such as hand lay-up for composites or forming for metals limits iterative design. An excellent form of prototyping is 3D printing, as it is cost-effective, fast, and flexible [14]. Additive manufacturing enables the production of complex geometries that are difficult to achieve using traditional manufacturing processes and has the flexibility of modifications for iterative design. Additive manufacturing can be used to compare the performance of different corrugated core geometries under diverse loading conditions.

Corrugated core sandwich panels are widely used within the construction industry due to their mechanical performance. Depending on their specific application, these panels are subjected to various types of loads, including bending, compression, and local impact, influencing their structural behavior and performance [15]. Panels with load-bearing and insulation abilities not only provide the necessary strength to support the weight of the structure but also help improve energy efficiency, soundproofing, and cost. The use of one panel with both capabilities can reduce the overall cost and environmental impact by minimizing the need for additional components.

Corrugated core sandwich panels are commonly used for load-carrying applications such as roofs and exterior walls, while foam core panels are used for sound, moisture, and thermal insulation [16]. As a result of the open channel design of corrugated core panels, they can be filled with foam for better insulation capacity. Various types of foams are used in sandwich panels, such as polyurethane (PU), Polystyrene (PS), and Phenolic. Different foams offer a combination of properties such as lightweight, high compressive strength, thermal and acoustic insulation, moisture resistance, and fire resistance [17,18]. Polyethylene Terephthalate (PET) foam, which is a closed-cell thermoplastic foam, is being extensively used in aerospace and construction industries in wind turbine and prefabricated insulated building structures. Despite the low density, PET foam offers high mechanical strength as well as resistance to environmental factors and cost efficiency. PET foam is an excellent choice for insulation panels due to its acoustic, moisture, and thermal resistance, as well as recyclability [19].

Due to environmental concerns, research is steadily shifting towards eco-friendly and recycled or recyclable materials. This trend is evident in the engineering field, where researchers are exploring sustainable design approaches that prioritize recyclability and material efficiency [20]. PET foam is highly recyclable as it can be reused and has a lower carbon footprint compared to other materials as it requires much less energy, leading to less environmental impact. PET plastics can be recycled and repurposed into packaging and construction supplies which helps reduce waste and consumption of raw material. PET recycling typically involves collecting and sorting items, cleaning the sorted material to remove contaminants, shredding, and pelletizing, after which the PET pellets can be reused to manufacture new products [21,22]. By adding recycled PET foam infills inside the corrugated core sandwich panels, a structure with good mechanical properties is combined with insulation, creating a sustainable and environmentally friendly product.

1.2 Aims and Objectives

This study is conducted to compare the performance of corrugated core sandwich panels with different geometries under compression and bending and to understand the strengths and weaknesses of each of the geometries. Furthermore, the effect of foam infill on the behavior of the samples under compression and bending is investigated. The core topologies under investigation are triangular, rectangular, trapezoidal, and circular. The samples will be created using additive manufacturing for rapid prototyping and iterative design. The recycled PET foam that will be used as an infill in this research is ARMAPET, with a density of 80 Kg/m^3. Later, a finite element model will be created to replicate the experimental results of compression and three-point bending with different corrugated core geometry. This model predicts the response of the different core topologies, including variables such as formation, stress, strain, and energy absorption. Numerical modeling not only facilitates a more in-depth understanding of the performance of each geometry but also provides a foundation for future research aimed at optimizing core geometry. Core optimization can be achieved by systematically investigating the impact of specific changes in the geometry, such as cell wall thickness and corrugation angle, on the mechanical performance of the panel.

The novel aspect of this study is its use of additive manufacturing and comparison of the different core topologies under compression and bending using the same exact dimensions of the unit cell. This will help us understand not only the capabilities of additive manufacturing and the prospect of PLA sandwich panels but also the use of PET foam integrated with an optimum core geometry to create a multifunctional panel that can accomplish two tasks simultaneously.

1.3 Thesis outline

Comprising a comprehensive thesis centered on the “Mechanical Performance of Foam-Infilled 3D-printed Corrugated Core Sandwich Panels: Experimental and Numerical”, this study is structured into five chapters, each defining a particular aspect of the research. The outline for each chapter is presented below:

Chapter 1: Introduction

Chapter 1 serves as an introduction to the study, providing detailed background on sandwich structures. It focuses on corrugated core geometries, emphasizing their importance and the need for further investigation in this area. This chapter also establishes the purpose of the study, focusing on applications and environmental impact. By laying this foundation, the stage is set for a deeper exploration of this topic and provides the necessary context for understanding the significance and direction of this research.

Chapter 2: Literature Review

Chapter 2 comprehensively identifies and analyzes the most relevant and significant research pertaining to the topic, thereby establishing a robust justification for this study. This chapter commences with an introduction to the general problem, providing contextual background and highlighting the need for further investigation. It then proceeds with a structured, in-depth discussion outlining the specific areas of research that are directly relevant to this work. By critically examining prior studies, this chapter emphasizes the importance of addressing unresolved questions and demonstrates how the current research builds upon and extends the existing body of knowledge.

Chapter 3: Methodology

Chapter 3 provides a detailed account of the design rationale underpinning the core geometry, highlighting the key considerations that influenced its structural configuration and layout. It delves into a discussion of the materials selection, examining their mechanical properties and the reasoning behind their suitability for the intended application. The chapter also outlines the experimental procedures in a step-by-step manner, describing the sample preparation, testing setup, and data collection techniques used to evaluate the mechanical performance of the core structures. Additionally, it elaborates on the numerical analysis methods employed, detailing the modeling approach, boundary conditions, meshing strategy, and simulation parameters applied to replicate the experimental conditions.

Chapter 4: Result and Discussion

Chapter 4 presents and analyzes the findings from the experimental and numerical investigations, providing insights into the compressive and bending performance of diverse corrugated core geometries. The chapter begins by summarizing the testing conditions and key results, followed by a detailed examination of the mechanical behavior of each core structure under compressive and bending loads. It compares the load-bearing capacities, failure modes, and overall structural performance of the different designs with and without foam infill. These findings highlight the variations in performance and offer a deeper comprehension of the deformation mechanisms and failure behavior, forming a foundation for further analysis and design optimization.

Chapter 5: Conclusion, Contribution, and Future Works

This chapter presents a comprehensive summary of the key research findings, focusing on how the core geometry impacts the performance of corrugated core sandwich panels. It highlights the influence of different core designs and the addition of foam on compressive and bending performance. Additionally, the chapter provides suggestions for future research that could build upon these findings and address remaining gaps in knowledge.

Chapter 2: LITERATURE REVIEW

2.1 Sandwich structures

Due to the popularity of sandwich structures, much research has been undertaken to understand their performance and optimize their use for different applications. Research on the mechanical behavior of sandwich panels covers a wide range of aspects, such as core design optimization, material selection, manufacturing processes, and failure mechanisms [23]. In recent years, corrugated core structures have gained considerable interest due to their ability to significantly improve energy absorption when a suitable geometry is chosen [8]. Numerous researchers have concentrated on a specific geometry of the corrugated core, examining and optimizing it. The core of sandwich panels is mainly loaded in compression and shear and is typically designed to minimize weight either through material selection or topology [2]. Since corrugated core sandwich panels have good impact resistance capabilities, many researchers have focused on this aspect. Wentao et al. [24], and Dolati et al. [25] investigated the low-velocity and high-velocity impact testing of trapezoidal cores, respectively, while et al. [26] examined the dynamic response of near-field air blasts of triangular cores. Having said that, impact has not been the only focus, and other work has been done on a single corrugated geometry, investigating it under tensile displacement [27], vibration dampening [28], and compression [13]. In addition to evaluating the common core geometries, many researchers have explored hybrid corrugated core designs such as trapezoidal-triangular hybrid and layered corrugated hybrid core designs and investigated their mechanical response, weight, and manufacturability [29-32].

2.2 Corrugated core sandwich panels

Research studies mentioned above clearly indicate that the corrugated core geometry significantly influences the performance of the panel under different loading conditions. In recent years, a growing effort has been made to determine the optimal core geometry. To do so, researchers have chosen different corrugated core topologies and evaluated them to compare their performance under mechanical loading, high temperature, etc [33]. Previous work on the bending and compression performance of corrugated panels shows interesting results. Xia F. et al. [34] compared corrugated panels made out of aluminum with cores of various shapes under longitudinal three-point bending, showing that rectangular has the highest load capacity, followed by trapezoidal, triangular, and sinusoidal. Abedzade et al. [35] evaluate the effect of core geometry on flexural stiffness and transverse shear rigidity of triangular, trapezoidal, and rectangular corrugated core sandwich panels made with woven glass fiber using vacuum assisted resin transfer molding (VARTM). The results showed that the triangular core has the highest flexural load capacity with the least amount of deflection. Although trapezoidal and rectangular showed less load-carrying capacity, they were capable of withstanding 5 times more deflection. Corrugated structures show an anisotropic behavior because the corrugated geometry creates a series of reinforcements along one direction, making the material resist deformation in the transverse direction, while in the longitudinal direction, the structures lack similar reinforcement, making the structure more flexible. This property of corrugated cores has been utilized in many designs, such as morphing wings, where the structure is desired to be stiff in one direction but flexible in the other [36]. Furthermore, Yu R. et al. [37] investigated the response of five different core geometries under minor energy impact and high energy impact, as well as compression. It was determined that Trapezoidal and rectangular had the highest load capacity before buckling, respectively, while arc-shaped and sinusoidal cores exhibited the lowest strength.

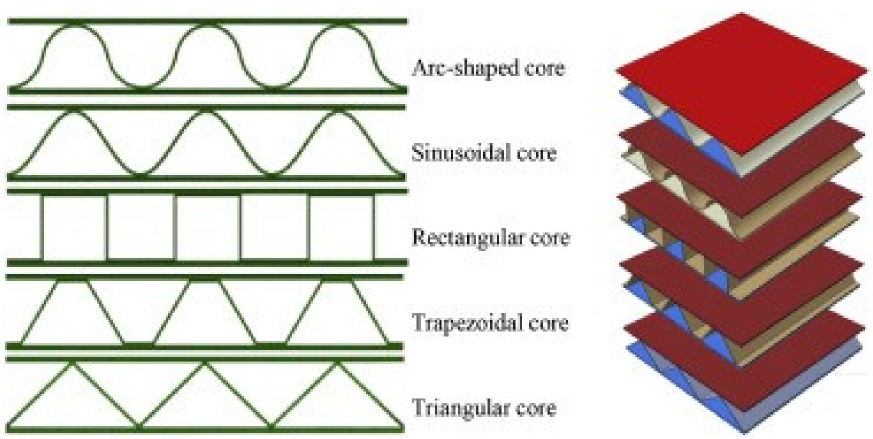

Figure 2.1. Axonometric drawing and core section of
five different geometries of corrugated core sandwich panels [37]

2.3 Additive Manufacturing

As previously stated, one of the main challenges of the comparative study of corrugated core topology is the sample manufacturing process. Since traditional manufacturing processes are time-consuming, costly, and lack customization and design flexibility, additive manufacturing has gained popularity in research. Additive technologies exhibit fundamental advantages, such as the possibility of producing complex microstructures with superior impact energy absorption capabilities, which cannot be made with standard manufacturing processes. As a result, this manufacturing technique has been studied to develop high-efficiency shock absorber cores [38], [39]. Many researchers have utilized additive manufacturing methods for development research, including the optimization of corrugated core geometry [40]. Iranmanesh et al. [41] investigated the effect of variation in core geometry on the structural performance of sandwich panels using 3D printing.

This study assessed different geometric configurations such as honeycomb, lattice, and custom-design structures to evaluate their impact on properties such as stiffness and strength, providing valuable insight into optimizing sandwich panel designs. As the use of 3D printing in the field of research grows, more studies focus on the possible benefits and weaknesses of this manufacturing method. For instance, the common materials used in 3D printing, such as PLA, ABS, and TPU, are isotropic, while the components 3D printed using these filaments show a degree of anisotropy. This is due to the layer-by-layer fabrication process creating a component that is strong along the printed layers and weaker between layers [42-44]. This nature of 3D printing can allow samples to be created with tailored properties as the anisotropy of the material can be controlled using the print orientation and infill patter. That being said, factors such as this must be thoroughly understood and considered to ensure accurate results during research. Other factors affecting the final property of 3D printed materials are design and print parameters such as print speed, infill, and layer height, which have been studied and explained in the sample preparation section [45].

2.4 Foam-filled sandwich panels

Honeycomb and corrugated core sandwich panels are mainly used for structural purposes due to their excellent mechanical properties. Foam-filled honeycomb core structures are widely used in industrial applications due to their multi-functional use. Many researchers evaluated adding foam to honeycomb core panels to improve stiffness and strength, energy absorption, and insulation [46-48]. Foam filling adds complexity to the manufacturing process by increasing the number of steps and the required equipment, which in turn raises the overall production cost. In the case of corrugated core sandwich panels, due to their open channel design, the structure can more conveniently be filled with foam, creating great opportunities for the use of this multifunctional structure.

Foam cores are primarily used in critical engineering applications, such as aircraft, automobiles, buildings, and spacecraft, due to their lightweight and better crashworthiness capability [8]. The thermal-acoustic insulation of PET foam has been analyzed, and the results show that it is particularly effective and minimizes sound transmission, making it an attractive choice for applications requiring efficient insulation performance while promoting environmental responsibility [49]. Research shows that sandwich panels with 100% recycled PET foam core are moisture resistant, do not absorb water, and help maintain structural integrity and mechanical properties even in humid and wet conditions. This makes sandwich panels with recycled pet foam great for the marine environment, construction, and transportation [50,51].

With respect to foam-filled corrugated core sandwich panels, several numerical and experimental studies have been conducted on the impact and blast performance of a single geometry [52-54]. Corrugated core sandwich panels exhibited great impact performance due to their enhanced energy absorption capabilities. Research on these panels under other mechanical loading conditions, such as compression or bending, is limited. One study investigated the energy absorption of single- and double-layer corrugated cores with and without foam infill under quasi-static loading. Compression performance of samples showed that panels with single-core and foam infill cores outperformed pure foam panels and bi-core corrugated cores with foam infill [55].

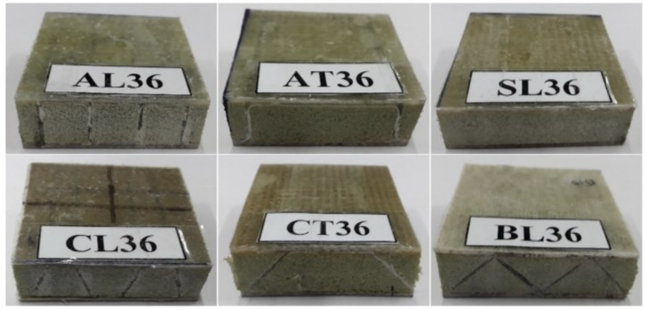

Figure 2.1. Foam-filled corrugated core sandwich panels with different core geometry [56]

Additionally, Taghizadeh et al. [56] studied PVC foam-filled corrugated core sandwich panels with rectangular, trapezoidal, and triangular geometries under planar, linear, and concentrated compression loading. The results show that rectangular and trapezoidal cores reach the highest load before deformation. Additionally, in this study, the effect of a number of corrugated channels on the property of the sandwich structure was evaluated, showing that the number of cells has a significant impact on the property. To the knowledge of the author no study was found to have compared the effect of foam infill on all the different corrugated core geometries investigated in this research. In addition, the performance of the panels under compression and bending was not shown before and after foam infill. By testing the hollow and foam-filled panels, we can investigate the improvement in strength and stiffness versus the increase in weight. Lastly, additive manufacturing was not utilized as a tool for comparison of various corrugated core topologies with anisotropic materials. This study aims to fill these gaps by investigating the behavior of rectangular, trapezoidal, triangular, and circular core geometries under compression and bending with and without foam core.

Chapter 3: METHODOLOGY

In this chapter, a detailed description of the procedures utilized to conduct the study will be provided. This will include an in-depth explanation of the design process for the core geometries, outlining the rationale behind the chosen configurations and dimensions. Furthermore, the sample manufacturing procedures will be described, covering the materials, fabrication methods, and measures implemented to ensure consistency and accuracy. Additionally, the material properties relevant to the analysis will be presented, along with the methods used to obtain these properties. Finally, the testing parameters and procedures will be thoroughly outlined, including the equipment setup, testing standards, and data collection techniques employed to evaluate the performance of the samples.

3.1 Core design

The mechanical properties of sandwich panels are significantly influenced by their core topology. This study examines and compares several core geometries, namely triangular, trapezoidal, rectangular, and circular designs. Studies have been conducted on optimizing the design of corrugated panels subjected to different loading conditions to minimize weight [57,58]. Researchers have strived to optimize the parameters of core geometry for a particular application manufactured using a specific material [59,60]. Unfortunately, there is no "one size fits all" solution to optimizing corrugated geometry. The refinement of geometrical parameters such as thickness of the panel, core walls, and skins or angles of a corrugated core sandwich panels depend on various factors, including material properties, loading conditions, and specific application requirements.

Researchers have found that thicker core walls can enhance compressive strength and stiffness but may increase weight. For instance, a study on the mechanical behavior of corrugated-core sandwich panels found that varying the cell wall thickness affected the compressive properties of the structures. Also, thicker skins can improve load-bearing capacity but may also contribute to increased weight. An optimal balance is necessary to achieve the desired mechanical performance without unnecessary weight addition [58].

The amplitude of the corrugation affects the overall load distribution and stability—larger amplitudes improve the energy absorption capacity and resistance to local buckling by enhancing the geometric rigidity of the core [61]. Meanwhile, the increase in the number of corrugations drastically affects the load-carrying capacity of the panels [56]. During the initial design of the corrugated core geometry, these optimization factors are used to create a well-conceived design.

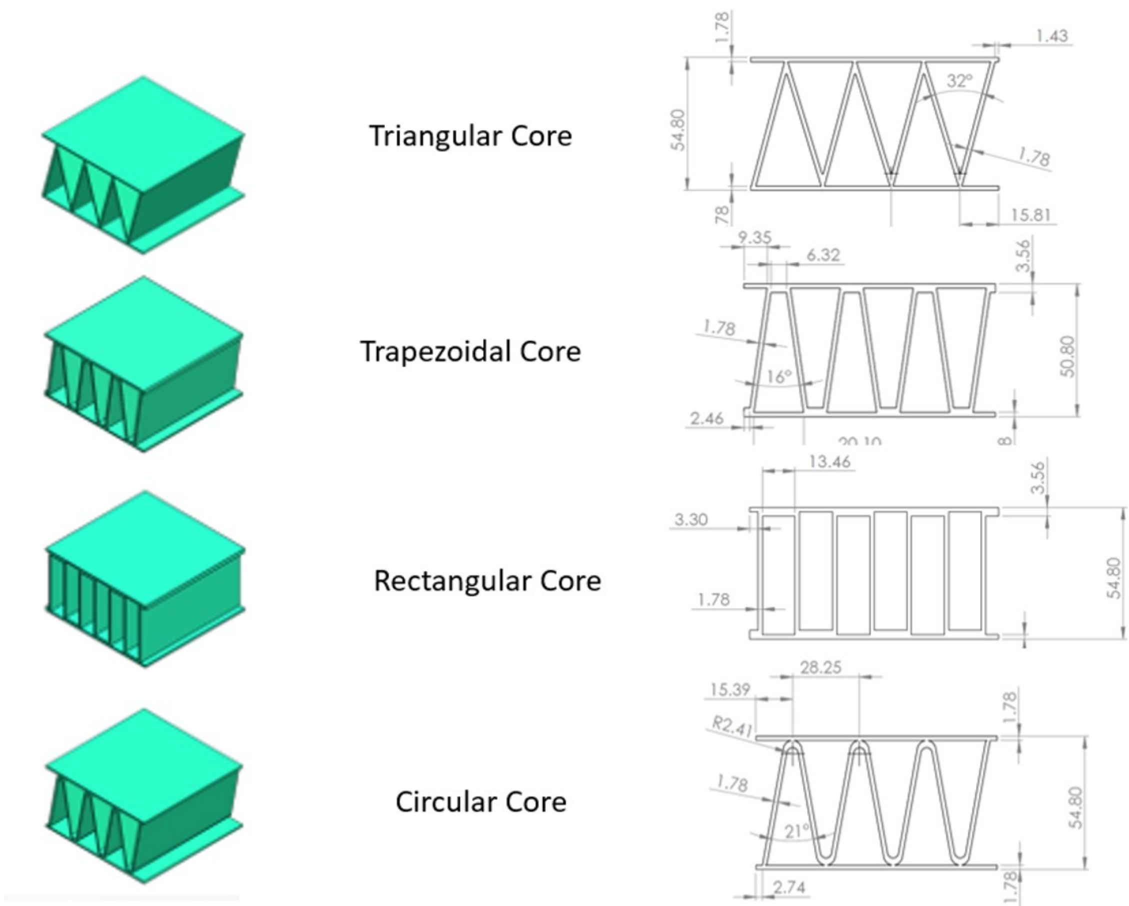

Figure 2.1. Isometric and front view with dimensions of the four corrugated core geometries

As this project is in collaboration with an industry partner, some of the dimensions are chosen in accordance with their products and applications. With that in mind, these dimensions are also considered to be within the optimum range. The thickness was chosen to be 2 inches as it is one of the standard panel sizes for insulation in the construction industry, and according to research, a larger amplitude is advantageous with regard to energy absorption and rigidity.

In building applications, the optimal total thickness of corrugated core sandwich panels is influenced by factors such as structural requirements, thermal insulation needs, and specific design criteria. The width and height of the compression and bending samples are limited by the size of the print bed and ASTM testing standards. The dimensions of the unit cells were devised so that each panel contained as many corrugation unit cells as possible while keeping the number of cells constant for every panel. The angles for the triangular, trapezoidal, and circular panel walls with reference to the horizontal line were kept between 45-85 degrees as angles smaller than 45 degrees were found by other researchers to have a significant impact on the load-carrying capacities. The thickness of the core wall and skins are chosen to be 1.78 mm, which is the thickness of the face sheets used by our industrial partner. Any of the dimensions mentioned above may be subjected to change after the experimental and numerical evaluations. The design and drafting process of the samples was performed on SOLIDWORKS so that a 3D model could be obtained to manufacture the samples.

3.2 Sample preparation

3.2.1 3D printing

After the design of the cell geometry was finalized, the samples were drafted on SOLIDWORKS. The sample files were later imported on a slicer software to generate g-code for the 3D printer. The samples were manufactured on a Prusa MK3 3D printer, recognized for its reliable performance, with a 0.4 mm nozzle and a direct drive extruder system. This 3D printer operates on Fused Deposition Modeling (FDM), also known as Fused Filament Fabrication (FFF). In this method, a thermoplastic filament such as PLA is fed into the hot end, after which the melted filament is extruded onto the print bed. Each layer is fused with the previous one as it cools, forming the final 3D printed object [62].

A slicer software is an important tool in 3D printing that converts 3D models into G-code, which is a form of instructions that the 3D printer can understand. During the slicing process, various parameters can be adjusted to optimize the printing process based on project requirements, whether the focus is on quality, speed, or specific mechanical performance. Some of these parameters are layer, infill, support, adhesion, speed, and temperature settings. The parameters used to print all the samples in this research are listed in Table 1.

Although all these parameters affect the quality of the final part, the critical factor in this project is to keep all the parameters constant throughout the manufacturing process.

Table 1. 3D-printing parameters

PRINTING SETTINGS	
NOZZLE TEMPERATURE	210 C
BED TEMPERATURE	60 C
RESOLUTION	0.2 mm
SPEED	70 mm/s
INFILL PERCENTAGE	100%
INFILL PATTERN	Lines
SHELL THICKNESS	0.8 mm

The nozzle and bed temperatures were set to 210°C and 60°C, which is on the higher end of the temperature range for PLA. However, this setting improves interlayer adhesion, facilitating the printing of smaller patterns more effectively and enhancing the adhesion of the sample to the print bed. The resolution refers to the precision and detail with which the printer creates the layers, which can affect the surface finish and sharp corners of the sample. Although resolution can be influenced by factors such as speed and nozzle diameter, the specific variable called "resolution" in the slicer software refers to the layer height. A resolution of 0.2 mm means that the thickness of each layer of material deposited by the 3D printer is 0.2 mm. This layer height was found to be a good balance between the print speed and quality of the sample, providing a reasonable surface finish while keeping the sample manufacturing at a reasonable pace.

Print speed is a variable that is dependent on the specific printer and material, but in this case, a speed of 70mm/s was deemed to balance quality and speed. Although lower print speed can improve print of the finer details, and as the print speed increases, the probability of introducing defects will increase, a long print time can also have adverse effects on the quality of the sample. Each compression sample took over 15 hours, while the bending samples required more than 30 hours, all printed at a speed of 70 mm/s. Longer print time can overheat the printer components, accumulate errors, create cooling problems, and offset the printer's stability.

The infill percentage in 3D printing refers to the percentage of the total volume of the object. In this research, 100% infill was chosen considering that the application of the sandwich panels under study is as structural components that require maximum strength. An infill pattern in 3D printing is a layout used to fill the internal structure of an object, offering a varying balance of strength, speed, and material usage. The line pattern, consisting of straight lines running parallel or at an angle, was selected to support the overall integrity of the panel while avoiding stress concentration areas in the sharp corners, a potential issue with other patterns like concentric. Additionally, some infill designs are specifically intended to enhance the strength of the sample, but their lack of uniformity can introduce uncertainty in research. Figure 3.2. is a preview of the shell and infill pattern of the rectangular compression sample.

Shell thickness refers to the number of outer layers printed around the premier of the object. Shell thickness was set to 0.8 mm to create a continuous print through the entire corrugated core. The continuous deposition of layers improves load distribution and prevents the formation of stress concentration areas. For instance, if the shell print stops at the end of the vertical wall and then begins again horizontally, this discontinuity can create a small void, leading to stress concentration in that area.

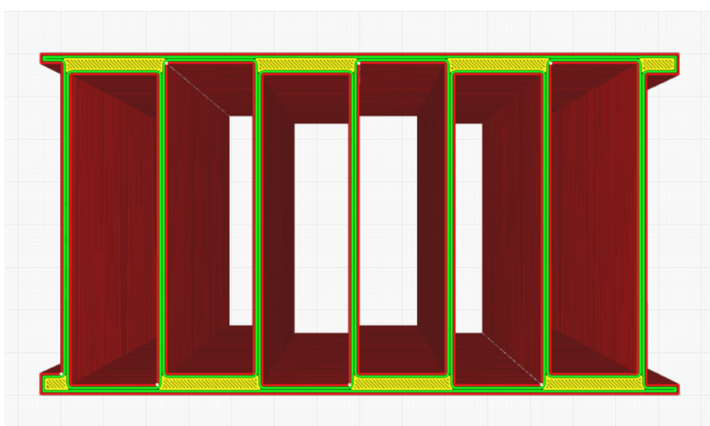

Figure 3.2. Preview of the corrugated core sample showing the printing pattern

It is important to note that during printing, the adhesion of the sample to the print bed was found to be insufficient due to the small surface contact area. Therefore, a layer of masking tape was added to the surface of the bed to increase friction and improve the grip between the sample and the bed.

3.2.2 PET foam infill

The foam inserts were cut out of larger panels using a circular saw a hotwire cutter. Before cutting the foam, 2D templates of the different geometry of the corrugated cells were compiled using the SOLIDWORK models created for 3D printing. To accommodate the adhesive and ensure an adequate amount is applied between the foam and the corrugated wall, a clearance was incorporated into the design before the template was printed. The most effective method found to cut large panels of PET foam was to use a circular saw with a carbide blade and a stream of water to prevent dust and foam particle circulation. For smaller, more intricate cuts with rounded edges, a hot wire cutter proved highly effective as it offered precise control, allowing for clean and detailed cuts. Additionally, the hot wire cutter produced smooth edges, preventing any crushing or compression of the foam, which can often occur with other cutting methods. This made it ideal for maintaining the integrity and quality of the foam while achieving the desired shape. It is relevant to note that the temperature and tension of the hot wire cutter and the feed rate of the foam each play an important role in the size and surface quality of the result. After all the foam inserts were cut for each sample, they would be inserted into the channel without adhesive to verify the size and geometry.

The PET foam inserts are bonded with the corrugated channels using a polyurethane liquid adhesive, ADBOND 5645. This adhesive is used in the industry to bond pieces of foam together as it expands, filling the open cells on the surface and thereby creating a strong bond. The adhesive is applied to all edges of the foam cutouts that are in contact with the corrugated core and the skins, and then a mist of water is sprayed over the adhesive before sliding them inside the corrugated channels. Since this adhesive is fast-acting, this process is performed one sample at a time. After all the foam pieces are inserted into one of the samples, two open ends of the corrugated channels are taped to prevent the adhesive from seeping through the gap. Next, the assembly is placed edge down, and a heavy steel plate is placed on top to apply pressure for better bonding, prevent the adhesive from leaking, and keep the foam pieces stationary, as the pressure created by the expanding adhesive will try to drive the foam out of the channels. The assembly is left for 24 hours to fully cure before removing the tapes and plate.

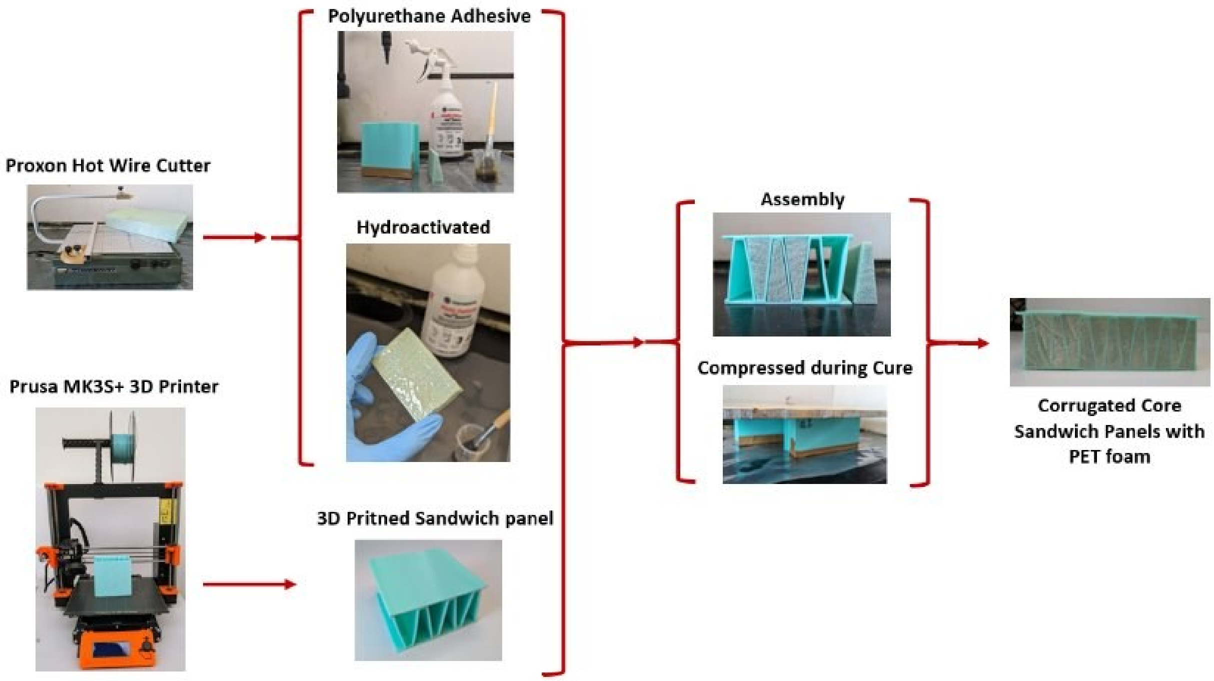

Figure 3.3. Steps of the sample fabrication process with and without foam infill

Figure 3.3 presents a graphical summary of the sample fabrication process. The compressive and bending samples, featuring corrugated cores with various geometries, were 3D printed. PET foam inserts were shaped using a hot wire cutter for the foam-infilled samples and bonded with a hydro-activated, expanding adhesive. Throughout the process, efforts were made to maintain consistency in each step to minimize the introduction of any manufacturing errors.

3.3 Material Properties

In any research, it is important to not rely on data sheets and to test the samples and obtain the properties. The material properties can help with the characterization of the material to predict and understand its response to testing. Later on, for numerical analysis on ABAQUS, the mechanical properties will play an important role. In this research, two main materials are used for sample preparation, which are polylactic acid (PLA) filaments and recycled polyethylene terephthalate (PET) foam. PLA is used in this study due to its ease of printing, dimensional accuracy, non-toxicity, and recyclability. All the hollow samples tested during this research can later be repurposed with the help of the Concordia Precious Plastic Project (CP3).

3.3.1. PLA Tensile Properties

Many factors affect the final property of a 3D-printed component. Some of those factors can be controlled such as print parameters and design parameters, for example, nozzle temperature, print speed, layer height, flow rate, cooling speed, orientation, and infill pattern. But there are also factors that are harder to control such as environmental and hardware factors. The type and environment of the 3D printer can significantly affect the properties of printed parts [63,64]. All the print and design parameters are kept constant through out this research. Since during testing the load will not always be applied with the same angle to the print direction samples are tested in multiple orientations for a more accurate analysis. The unprocessed PLA is shown to have better tensile properties compared to the 3D printed PLA due to the defects introduced during the additive manufacturing process. Studies performed on this subject found the raw PLA has a tensile strength of 60 MPa, while 3D printed PLA has a lower tensile strength of 48 MPa [65,66].

The properties of PLA are found in accordance with the ASTM D638-22 [67] Standard Test Method for Tensile Properties of Plastics. For the tensile test, three specimens with three print directions of 0°, 90°, and ±45° were printed with PRUSA MK3S+. According to the standard, the dog bone sample type IV dimensions can be seen in Figure 3.4. The specifications of the filament used, and the print parameters can be seen in Table 2.

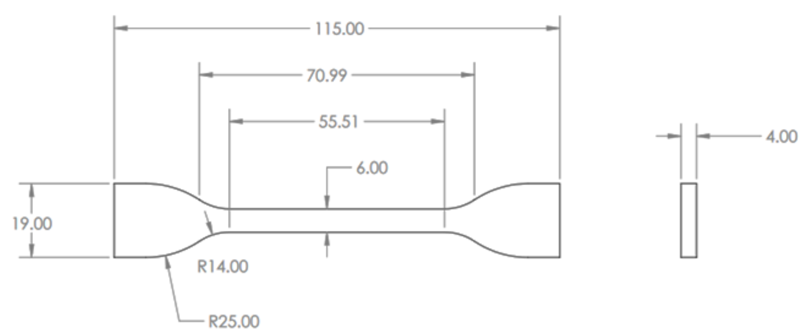

Figure 3.4. Tensile test specimen type IV dimensions (in mm) in accordance with ASTM D638-22 standard

Table 2. 3D printing filament specification

FILAMENT SPECIFICATIONS	
DIAMETER	1.75mm
TOLERANCE	+/-0.03
NET WEIGHT	1 KG
SPECIFIC GRAVITY	1.24 g/cm^3

As can be seen in Figure 3.5, the ±45° orientation specimens were printed horizontally lying flat on the print bed, the 90° specimens were printed standing vertically, and the 0° specimens were printed on the side. To print samples in 0 and 90-degree supports, rafts and masking tape were required for better adhesion due to the small surface contact areas with the bed.

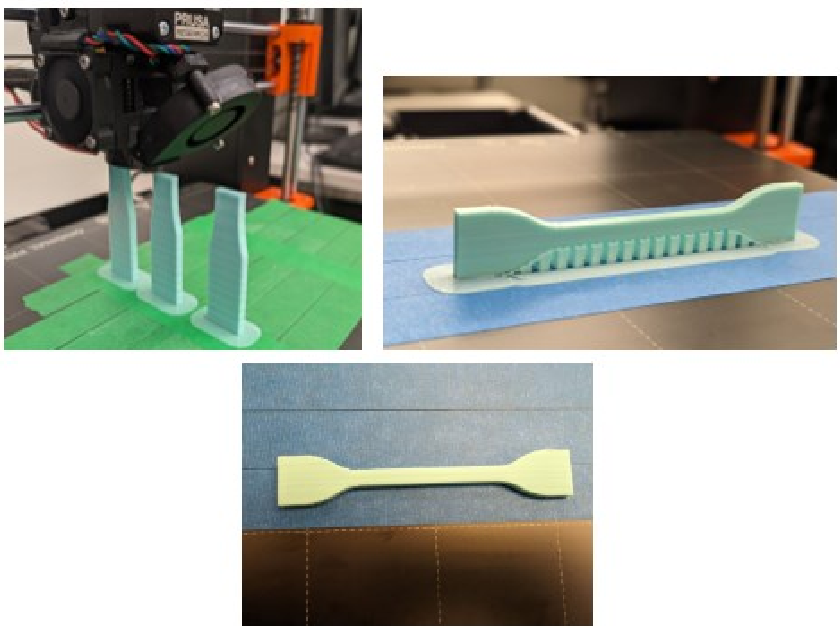

Figure 3.5. Tensile test specimens manufacturing. 90 degrees (Vertical), 0 degrees (On the side), and ±45 degrees (Horizontal)

The three different dog bone samples with different print angles can be seen in Figure 3.6 before and after failure. While the ±45° specimen has a smooth surface, the 0° - and 90° specimens have a slightly wavy surface texture. 3D printing part orientation can affect the surface finish of the final product, and although the surface finish can be improved by adjusting print parameters and machine settings, it would be counterintuitive in our study as we want to keep the parameters exactly the same to avoid introducing errors.

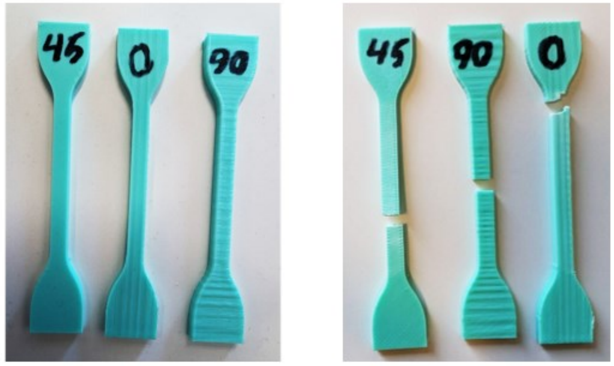

Figure 3.6. 3D printed samples of ±45, 0, and 90 degrees before and after the tensile test

Tensile tests were performed on the samples using a HOSKIN SCIENTIFIC tensile test machine, as shown in Figure 3.7, utilizing a 5Kn load cell with a 2mm/min displacement rate. It can be observed that the 90° samples had a sudden interlayer failure, but the ±45° and 0° samples were elastic until the yield point with a significant post-yield strain region. Due to the nature of defects in 3D-printed samples, the strain failure of each sample for each orientation was very different.

Figure 3.7. Tensile testing setup on HOSKIN SCIENTIFIC testing machine

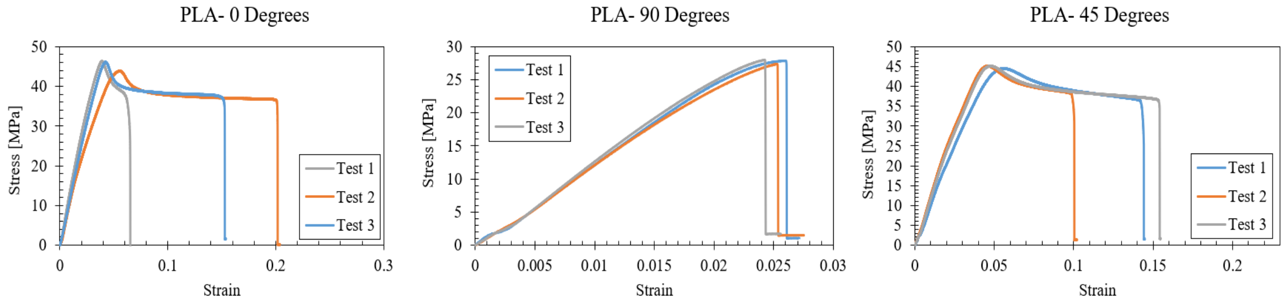

Figure3.8. Stress-strain curves of 3D printed PLA samples under tensile load

Table 3. Tensile properties of PLA

Property	**0°**	**90°**	**45°**
TENSILE STRENGTH	45.4 MPa	27.8 MPa	44.1 MPa
TENSILE Modulus	1.2 GPa	1.1 GPa	1.1 GPa
POISSON RATIO	0.33	0.33	0.33

As shown in Figure 3.8 and summarized in Table 3, the tensile properties of the specimens vary significantly across different print orientations. In the 0° orientation, the filament is aligned parallel to the applied load, allowing the stresses to be effectively distributed along the continuous filament. This configuration maximizes the tensile strength, which reaches 45.4 MPa. In contrast, the 90° orientation exhibits the lowest tensile strength of 27.8 MPa. This is due to the load being applied perpendicular to the printed layers, leading to failure primarily along the interlayer bonds. The specimens printed at ±45° orientation demonstrate an intermediate tensile strength of 44.1 MPa. In this case, the load is distributed across both the filament strength and interlayer adhesion, resulting in better performance than the 90° orientation but still weaker than the 0° configuration. The strain experienced by the 90° specimen before failure is much lower than the strain experienced by the 0° and ±45° specimens. When the print direction is aligned with the loading direction the material experiences a large degree of plastic deformation. However, when loading is perpendicular to the print direction, the samples fail due to weak interlayer bonding acting similar to brittle material. Notably, the tensile modulus does not exhibit substantial variation across orientations. Even with weaker interlayer adhesion, the initial stiffness of the material remains relatively consistent, with noticeable differences only occurring closer to failure. The properties obtained from this section will be utilized for finite element modeling.

3.3.2 PLA Compressive Properties

After the properties resulting from the tensile test were inserted into the ABAQUS models, the results showed that the strength of the material should be higher than what was obtained experimentally. It was previously recognized that due to the layered structure, anisotropy, and bonding mechanism, the mechanical properties of a 3D parts are direction dependent. It was further detected that if the print direction is perpendicular to the direction of the force, the layers will be pulled apart, and if they are parallel, cracks can propagate easily between the layers [68]. Due to these factors, compression is expected to outperform tension in 3D printed parts.

The compression properties of PLA are determined in accordance with ASTM D695-23 [69] Standard test method for compressive properties of rigid plastics. The samples are printed with the same design and print parameters in 0° - and 90° orientations. The fiber orientation has less effect on the compression properties compared to tensile, which is why ± 45° was removed. In Figure 3.9, the sample shape and dimensions for the compression test can be seen along with the 3D-printed samples. The longer sample is recommended to be used for obtaining the elastic modulus, and the shorter sample is to obtain ultimate strength without buckling.

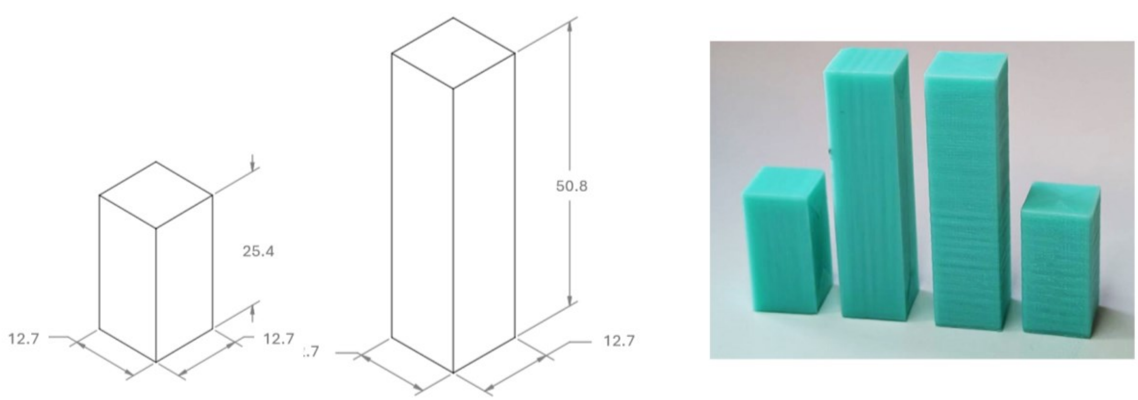

Figure 3.9. Compression test specimen dimensions (in mm) in accordance with ASTM D695-23 standard (left) and manufactured sample using 3D printing (right)

The results indicated no significant variation in the strength or elastic modulus between samples with the same orientation but differing heights. As a result, these samples were excluded from the subsequent graph for clarity and consistency in the analysis.

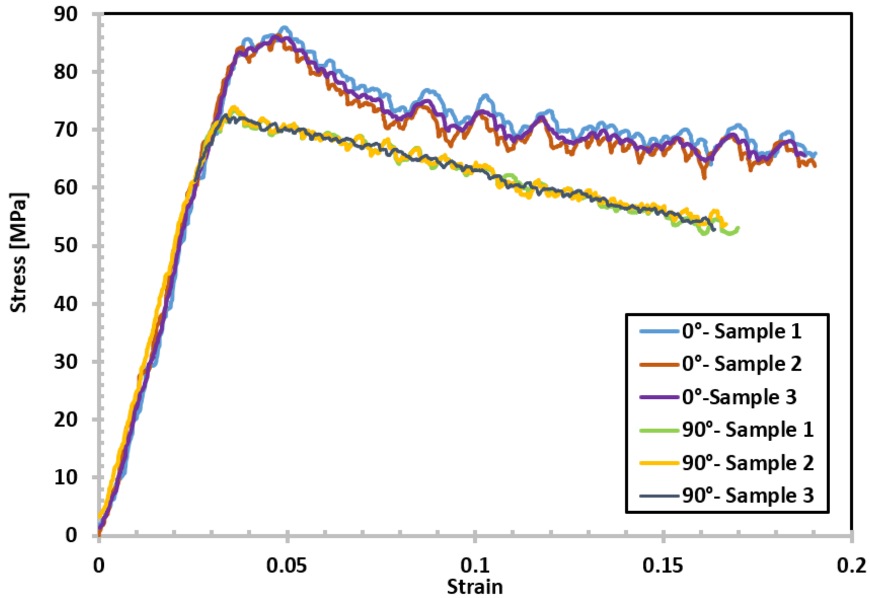

Figure 3.10. stress-strain curves of 3D printed PLA samples under compressive load

As shown in Figure 3.10, the elastic modulus of the 3D printed PLA samples are the same in 0° and 90° orientation, but the ultimate strength is higher in 0° samples. In compression, the print layers compact under the applied force and resist deformation, reducing directional dependence and leading to similar elastic modulus. The compressive strength of PLA at 0° is higher as the print layers are parallel to the print direction Since the load is distributed along the continuous path of extruded materials. While in 90° samples where the compression load is applied perpendicular to the printed layer the weak interlayer adhesion will create areas of stress concentration. A summary of the compressive properties of PLA can be found in Table 4.

Table 4. Compressive properties of PLA

PROPERTIES	**0**	**90**
COMPRESSIVE STRENGTH	86 MPa	72 MPa
COMPRESSION MODULUS	2.6 GPa	2.6 GPa
POISSON RATIO	0.35	0.35
YIELD STRENGTH	83 MPa	69 MPa

By comparing the compressive and tensile properties of PLA, it can be seen that, as predicted, the ultimate strength has almost doubled. However, the compressive modulus is subtly less than the tensile modulus. This is due to the alignment of the direction of load distribution, making the layers resistant to stretching due to continuous polymer chains. While the micro voids and interlayer gaps make the material become more flexible. This comprehensive analysis of the mechanical properties of PLA in tension and compression will assist in creating a more accurate finite element model.

3.3.3 PET Foam Properties

The foam used in this research is recycled polyethylene terephthalate foam from Armacell [70] which is a type of closed-cell thermoplastic foam. To manufacture foams, typically, the resin is melted, mixed with a blowing agent, and then extruded through a die. In the case of the r-PET foam used in this project, the die utilized to extrude the foam is a special multi-hole breaker plate, which results in a honeycomb-shaped foam block [71]. Due to the micro honeycomb structure of the foam, the compression properties of PET foam differ across the three directions. As a result of this, the compressive properties of r-PET foam samples are tested in three orientations. Additionally, the recycled PET foam is manufactured in rectangular segments and joined together to create a larger panel. Due to this, there is a weld line that runs across the panel every few inches, as can be seen in Figure 3.11. Since the material is heated, melted, and compressed to connect the two segments, the weld lines are denser and will, overall, reinforce the panel, making it stronger. To assess the impact of the weld line on the compressive performance of the panel, a group of samples without a weld line will be tested alongside a group of samples with a weld line.

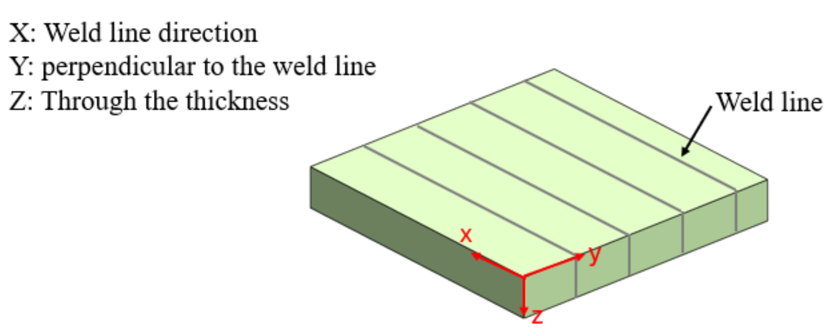

Figure 3.11. PET foam test coordinate system

To evaluate the compressive properties of the PET foam, a series of compression tests were conducted following ASTM C365 [72] standard. The samples of 25.4 mm x 25.4 mm x 25.4 mm were prepared using a hot wire cutter. Testing was performed on a universal MTS machine equipped with a 5KN load cell. The remaining test parameters can be found in Table 5To ensure the accuracy and reliability of the results, the compression test for each direction, with and without the weld line, was repeated three times. The fixture used for the compression test can be seen in Figure 3.12.

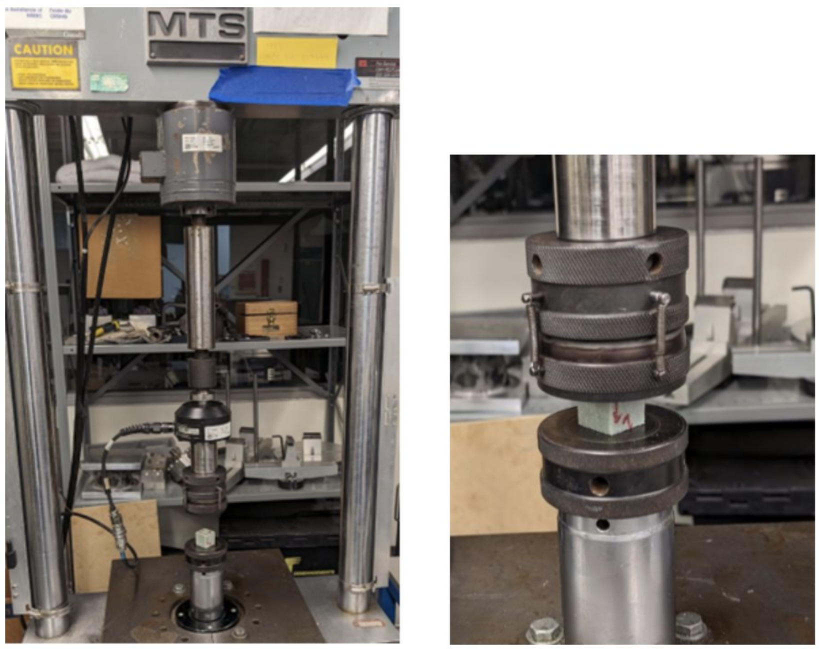

Figure 3.12. Flatwise compression testing setup of r-PET foam on universal MTS testing machine

Table 5. Test parameter for compression of PET foam

TEST PARAMETERS	**VALUE**
STANDARD	ASTM C365
SPEED	0.5 mm/min
TEMPERATURE	Room Temperature
LOAD CELL	5K
SAMPLE SIZE	25.4x25.4x25.4 mm
PRELOAD	45N
DATA RECORDING	2-3 data recordings per second

The results of the compression tests show that the foam has similar properties in the x and y directions, but as predicted, the strength significantly increases in the z-direction. Furthermore, since the weld line is parallel with the applied load during compression in the z-direction it strengthens the material. On the other hand, since the weld line is perpendicular to the direction of loading in the x and y direction there is no change in the material property.

As seen in Figure 3.13, the r-PET foam initially experiences a linear section followed by plasticity, where the foam cell walls start to buckle and be crushed. Within the plateau region foam cells deform and collapse under load without a significant increase in stress. This phenomenon shows cases of the energy absorption capability of foams. After most of the cells are crushed, we reach the densification region, where the stress will begin to climb again. The r-PET compression sample before and after testing can be seen in Figure 3.14. The sample in the z direction has a post-yield softening region that can be seen after the peak caused by the wall of the honeycomb structure. The same can be said for the sample in the z direction with the weld line, where the weld can be seen to have affected the plasticity peak and introduced more variation in the plateau region.

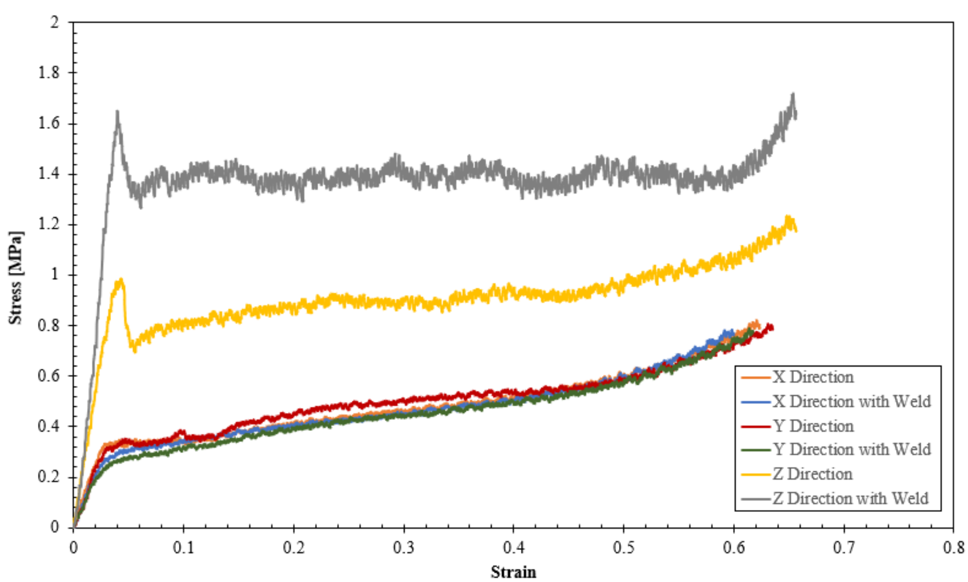

Figure 3.13. stress-strain curves of r-PET foam samples under compressive load

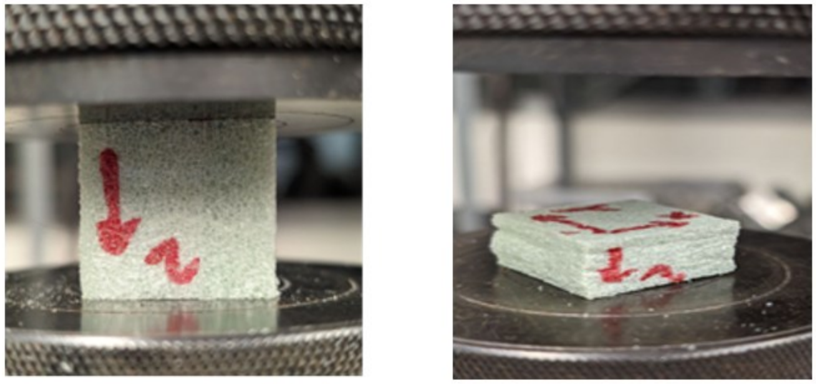

Figure 3.14. r-PET foam before and after compression testing

To ensure consistency and accuracy, all foam infills inserted into the corrugated channels were meticulously cut along the same axis, with no weld lines introduced. Given that the thickness of the PET foam matched that of the corrugated panels, the cutouts were made through the thickness to minimize waste and optimize load-bearing capacity. Consequently, the z-axis of the foam aligns with the direction of the applied load during flatwise compression and three-point bending tests. The table below presents a summary of the compressive properties of the recycled r-PET foam.

Table 6. Compressive properties of r-PET foam in z-direction

PROPERTIES	**PLA**
DENSITY	80 kg/m^3
COMPRESSIVE STRENGTH	1 Mpa
COMPRESSION MODULUS	22.8 MPa
POISSON RATIO	0.35

3.4 Experimental Procedure

3.4.1 Flatwise Compression Test

To evaluate the compressive strength of the corrugated core sandwich panels, a series of flatwise compression tests were conducted following the ASTM C365 standard. Samples of 101.6 mm x 101 mm x 50.8 mm with and without r-PET foam infill were prepared for the test. Testing was performed on an INSTRON 3400 machine equipped with a 100kN load cell, and the displacement rate was set to 2 mm/min. To ensure the accuracy and reliability of the results, the compression test for each of the geometries was repeated three times without infill and two times with r-PET infill.

The fixture used for flatwise compression consists of two circular platforms, as shown in Figure 3.15. The bottom platform is flat and has no degree of freedom, while the top platform consists of two parts that are held in place using 5 springs. The springs allow for three additional rotational degrees of freedom for the test fixture to adjust to any specimen imperfections, reduce bending moment, and ensure linear deformation during testing.

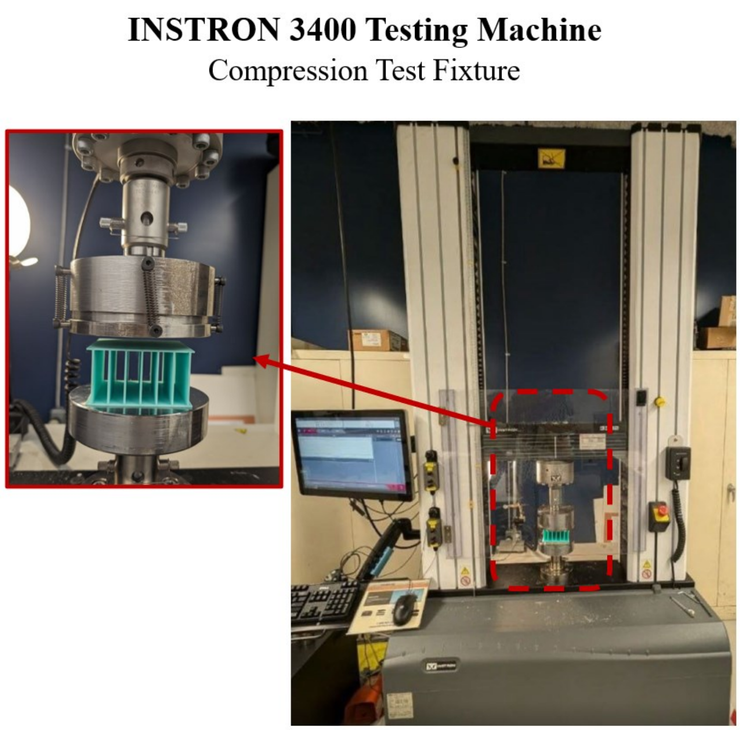

Figure 3.15. Flatwise compression testing setup on INSTRON 3400 testing machine

3.4.2 Three-Point Bending Test Procedure

To evaluate the flexural strength of the corrugated core sandwich panels in the transverse direction, a series of three-point bending tests were performed following the ASTM C393 [73] standard. For the test, samples of 203.2 mm x 76.2 mm x 50.8mm with and without r-PET foam infill were prepared. Testing was performed on a universal MTS machine equipped with a 100kN load cell, and the displacement rate was set to 2mm/min. To ensure the accuracy and reliability of the results, the three-point bending test for each of the geometries was repeated three times without infill and two times with r-PET infill.

The fixture used for three-point bending consists of two platforms that are aligned together using two rods attached to one fixture and two guiding bearings mounted on the other, as shown in Figure 3.16. This prevents the fixtures from slipping during testing. Two sliding supports are added to the bottom, and one is added to the top to apply force. The supports where the specimen rests and the force is applied have a rectangular shape and are 76.2mm x 20 mm. These rectangular plates rest on a cylindrical part and are held together by three springs on each side. Although the sample can also be placed on cylindrical supports to concentrate the load on a single line, it was decided that rectangular supports would be used. This decision was made because the position of the load can have a significant impact on failure, especially in hollow specimens with a small surface area connecting the core to the skin.

Universal MTS Testing Machine

Three-Point Bending Test Fixture

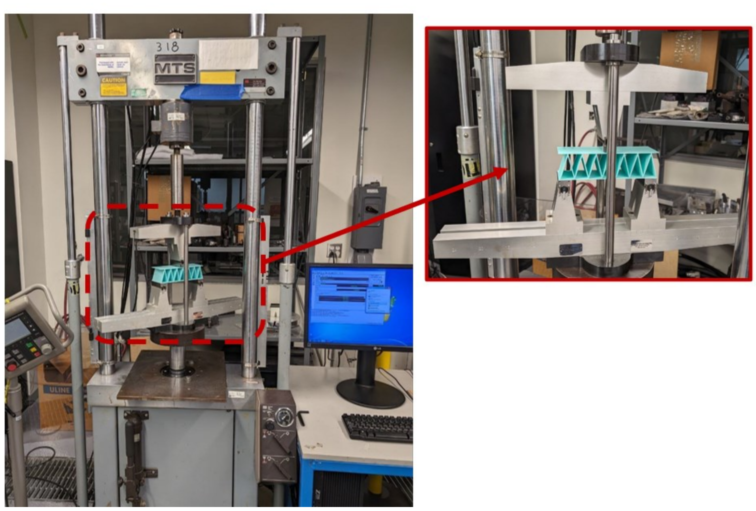

Figure 3.16. Three point bending testing setup on the universal MTS testing machine

3.5 Numerical Modeling

The finite element analysis of the corrugated core sandwich panels was conducted on ABAQUS software, which is capable of analyzing complex geometry and advanced material behaviors while providing comprehensive visualization tools. The development of the ABAQUS model consists of multiple essential stages ensuring precise and detailed simulations that can provide valuable insights into the performance of each core geometry under compression and bending.

3.5.1 Compression Modeling

The modeling process begins with importing the geometry from SOLIDWORKS on the ABAQUS platform and inputting the mechanical properties found in section 3.3. a fixture is then created and assembled on the top and bottom of the sample, one as a support and one as the compressor, as shown in Figure 3.17. Since the testing fixtures are made of stainless steel, which is much stronger than PLA, the fixtures are treated as rigid shells in the model. To simulate the interaction between the sandwich panel and the fixtures a surface-to-surface contact was incorporated. In modeling materials that may bend and fold, such as plastics, a self-contact must be set on ABAQUS. This prevents the nodes and elements from penetrating each other and maintaining physical accuracy. During the simulation, the top fixture will move in the negative y direction, and the force is recorded. The bottom fixture is fixed in place with no degrees of freedom, while the top fixture is allowed to move in the y direction only. These boundary conditions are set on a reference point on the rigid fixtures.

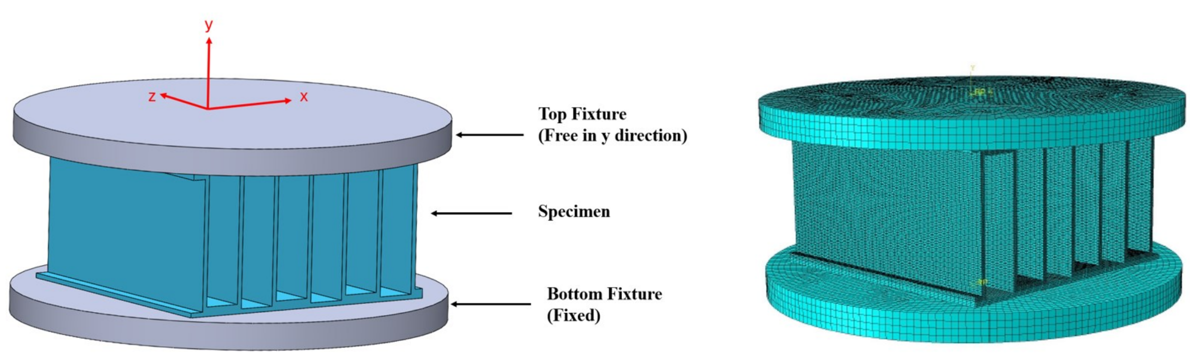

Figure 3.17. Finite element modeling for compression design part (left) and meshed part (right)

Furthermore, a mesh study was performed to achieve an optimal balance between simulation accuracy and mesh quality. This process involved refining the mesh to verify that the results remained consistent and were not notably influenced by changes in mesh density. It is important to note that in thin-walled structures, a small number of elements across the thickness of the wall can cause a coarse representation of the stress, producing inaccurate results. If the model has complex geometry and stress concentration areas, larger elements can cause unpredicted failure.

Another important factor in mesh study is the type of element used for the model. In this study, the hexahedral element was utilized for the two fixtures and the specimen. Hex element type is typically more computationally efficient, improves stress distribution, and reduces numerical errors in thin sections. It was confirmed that the hex elements mesh uniformly with the geometry and produced results that closely match the experiment. Our comprehensive finite element analysis, as outlined above, allows us to develop a thorough comprehension of the behavior exhibited by the corrugated core sandwich panels under compression and bending. This, in turn, supports our efforts to gain valuable insights into their performance attributes and failure mechanisms.

3.5.2 Bending Modeling

Consistent with the previous model, the process begins with importing the geometry from SOLIDWORKS and inputting the mechanical properties of PLA. A simplified three-point bending fixture is then designed and assembled with the specimen, as shown in Figure 3.18. The fixture includes three rectangular supports-two at the bottom and one centered on top. Since the testing fixtures are made of stainless steel, which is much stronger than PLA and is not expected to deform, they are treated as rigid shells in the model. The surface interaction is set similarly to the compression model, with surface-to-surface contact between the fixtures and their respective contact surfaces and self-contact between all the surfaces of the sample. During the simulation, the top rectangular fixture will move downwards in the y direction, and the forces are recorded. the two bottom fixtures that are used as supports are fixed in place with no degrees of freedom, while the top fixture can only move in the y direction. These boundary conditions are set at the reference point of each of the fixtures. The mesh study was previously performed for the corrugated geometry, and as such, the same elements were used in this modeling.

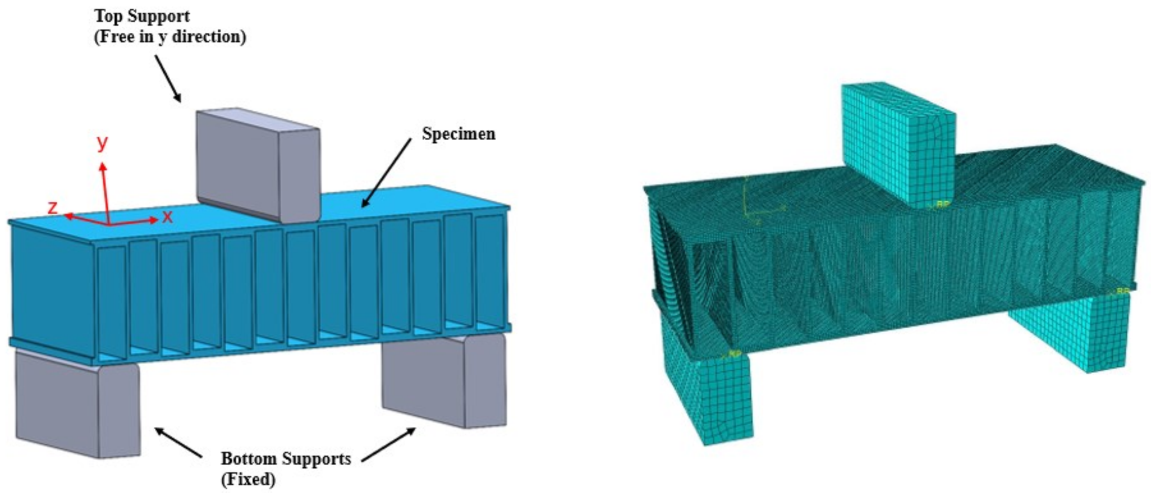

Figure 3.18. Finite element modeling for three-point bending design part (left) and meshed part (right)

It is important to understand that the perfect sample under ideal conditions that are examined during finite element modeling doesn’t always match the real-life scenario. This effect is even more predominant when studying buckling, collapse, or nonlinear behavior. No sample is perfectly manufactured and there are always deviations in size, geometry, and preexisting stresses. Samples manufactured using 3D printing contain microstructural imperfections such as voids and pores due to incomplete fusion between the layers. 3D printing processes such as FDM involve cooling, and heating cycles that cause residual stresses within the component. In structures such as corrugated core panels that are prone to buckling, perfect geometry can lead to unrealistic predictions. Adding imperfections to the modeling process can replicate manufacturing defects and initiate local deformation, causing realistic buckling mode to better reflect the actual performance of the panels.

Chapter 4: RESULTS AND DISCUSSIONS

In this chapter, the data obtained from the compression and bending tests are presented, and the response of each core geometry is assessed. The objective is to identify the relation between the core topology and the performance of the sandwich panels and examine their failure mechanism. Later, the results of the experimental and numerical analysis are compared with the numerical model, and insight into the internal stresses on the corrugated core and skins during compression and bending is obtained.

4.1 Effect of core topology on Compressive strength

Corrugated core panels with four different geometries were manufactured and tested under flatwise compression, as shown in Figure 4.1, which displays the samples before and after buckling. All the panels exhibit mode 1 buckling under compression, but the direction of buckling varies. The observed buckling pattern aligns with the expectation, showing variation in shapes and directions due to the random distribution of imperfections during 3D printing. The corrugated walls in all the panels were observed to initiate buckling simultaneously, while one of the walls in the rectangular core buckled before the rest, thereby disturbing the load distribution and causing all the buckling to happen in the same direction.

Triangular Corrugated Core Before and After Failure

Trapezoidal Corrugated Core Before and After Failure

Rectangular Corrugated Core Before and After Failure

Circular Corrugated Core Before and After Failure

Figure 4.1. Corrugated core samples under flatwise compression loading

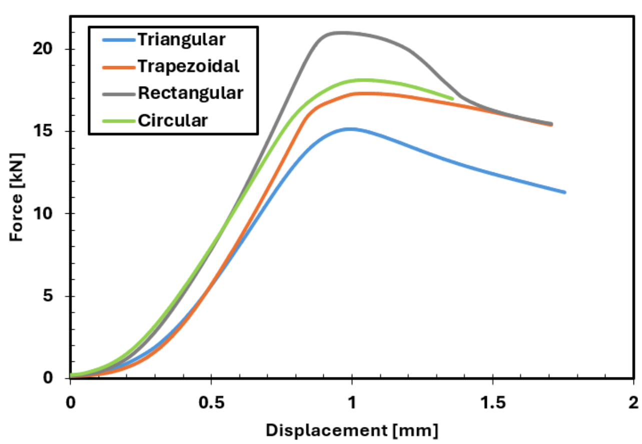

Figure 4.2. Force-displacement curves of the corrugated core panels under compression

The force-displacement graph shown in Figure 4.2 demonstrates an initial non-linear region caused by surface irregularities and distance between the layers deposited by the 3D printing process. After all the layers are compacted and the fixture has full contact with the sample's surface, a large linear region can be seen where the material is deforming elastically. When the graph starts to deviate from linearity, the panels undergo plastic deformation, which is followed by buckling. The peak of this graph represents the maximum load each geometry can carry before buckling. According to the data, the rectangular core exhibits the highest load-carrying capacity, whereas the triangular core demonstrates the least. The circular and trapezoidal cores ranked second and third in load capacity, respectively. However, their values were close enough that modifying the design parameters could potentially alter their rankings. The average of the numerical data obtained from the compression tests including the maximum compression force and the energy absorbed, can be seen in Table 7. As the panels do not have the same weight the normalized results are added for easier comparison.

Table 7. Summary of data under flatwise compression for Hollow samples

Core Geometry	Weight [g]	Max Compression Force [kN]	Energy Absorbed [N.m]	Energy Absorption to weight ratio	Max compression to weight Ratio
Triangular	126.7	15.15	6.56	0.052	0.120
Trapezoidal	132.9	17.33	7.98	0.060	0.130
Rectangular	146.7	21.00	8.61	0.059	0.143
Circular	133.4	18.14	9.34	0.070	0.136

4.2 Effects of core topology on bending strength

The corrugated core samples with four different geometries were tested under three-point bending, and the samples before and after buckling are shown in Figure 4.3. It can be seen that the triangular, trapezoidal, and circular panels experience a more localized buckling where the unit cell is directly under the top fixture buckles. The deformation is observed to spread across the unit cells closest to the center from both sides. In contrast, the rectangular sample underwent global buckling of the structure. Unlike the other three samples, which experience rapid buckling failure, all the corrugated walls of the rectangular sample begin to buckle simultaneously. However, the deformation of the structure prevents further buckling.

Triangular Corrugated Core Before and After Failure

Trapezoidal Corrugated Core Before and After Failure

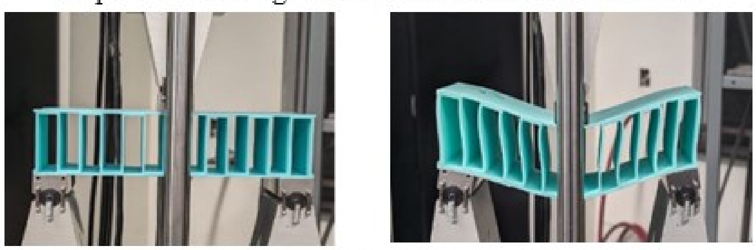

Rectangular Corrugated Core Before and After Failure

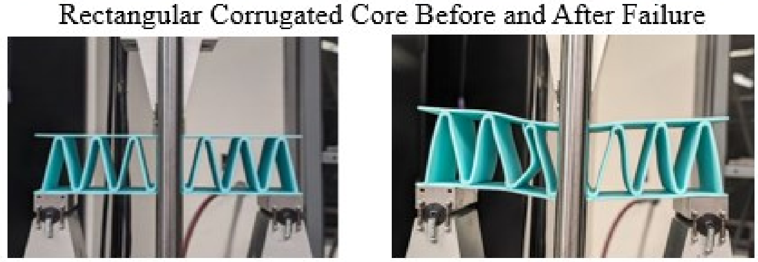

Circular Corrugated Core Before and After Failure

Figure 4.3. Corrugated core samples under three-point bending load

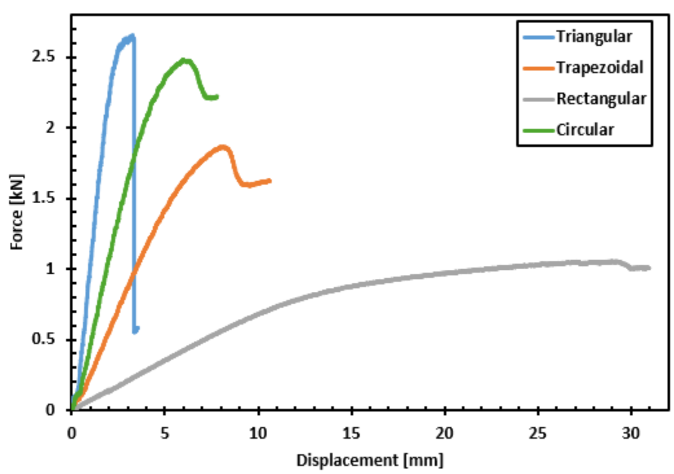

Figure 4.4. Force-displacement curves of the corrugated core panels under three-point bending

The force-displacement graph shown in Figure 4.4 demonstrates an initial linear section where the structures experience elastic deformation. This is followed by a deviation from linearity, indicating the onset of plastic deformation. After the plastic region, the corrugated core begins to buckle. It is observed that the triangular core buckling leads to a quick fracture failure, which is caused by stress concentration at the intersection of the core with the skin. Meanwhile, the circular and trapezoidal cores experienced a more controlled buckling failure. It is also evident that when the rectangular core enters the plastic region, the entire structure experiences global buckling, leading to a large displacement. According to the summary of data shown in Table 8, the triangular core experienced the highest flexural load capacity, followed by circular and trapezoidal. The energy absorbed by each corrugated panel during bending is calculated until the point of buckling failure. It is important to note that the large energy absorption of the rectangular core is due to the large displacement caused by global buckling. Since this panel had a different failure mechanism, it can not be compared with the rest regarding energy absorption.

Table 8.Summary of data under three-point bending for Hollow samples

Core Geometry	Weight [g]	Maximum Force [kN]	Energy Absorbed [N.m]	Energy Absorption to weight Ratio	Max Force to weight Ratio
Triangular	182.8	2.66	4.91	0.027	0.015
Trapezoidal	197.1	1.86	8.75	0.044	0.009
Rectangular	212.0	1.06	21.20	0.100	0.005
Circular	196.2	2.48	8.78	0.045	0.013

4.3 Effects of Foam infill on Compressive strength

In this section, the four different corrugated core geometries with PET foam infill are tested under flatwise compression, with Figure 4.5 showing each of the panels before and after failure. Similar to the results of the compression test on the hollow panels, the samples failed due to buckling. However, with the addition of the adhesive and PET foam, other types of failure modes were also observed. The direction of the buckling and location of failures are determined by manufacturing irregularities from the 3D printing process, foam infill, and the adhesion of the foam to the corrugated walls. Additionally, in contrast to the hollow samples, a more severe form of brittle failure was observed, where the corrugated wall either fractured in the middle or broke off entirely.

Figure 4.5. Corrugated core samples with foam PET infill under flatwise compression loading

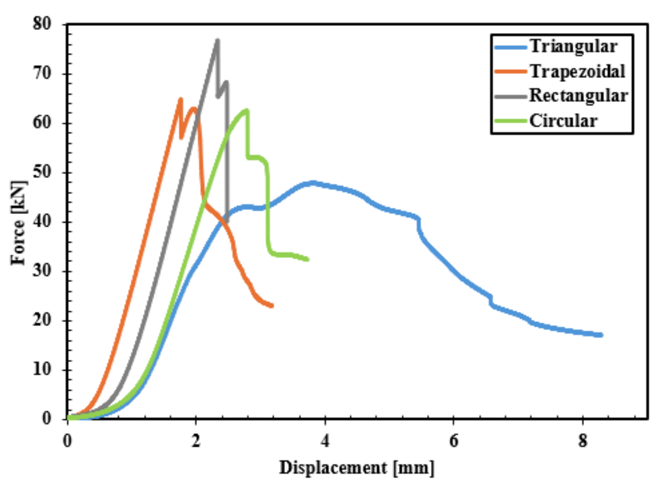

Figure 4.6. Force-displacement curves of the corrugated core panels
with PET foam infill under compression

The force-displacement graph of the corrugated core panels with PET foam infill can be seen in Figure 4.6. Similar to compression without the foam, the graph starts with a small curve where the fixture has yet to fully contact the surface, and the 3D-printed layers are flattened on one another. After the initial linear-elastic region, a sharp peak is created due to the shear failure of the adhesive used to assemble the core to the skin. After the drop, the forces increase again, showing plastic deformation followed by buckling failure. Following buckling, the walls crush the foam in some locations, causing cell wall collapse and densification. Due to the densification of the PET foam, a subtle flattening of the load can be seen before a final failure, which was observed to be a combination of brittle fracture of the foam and fracture of the corrugated core. The summary of the data from this test is shown in Table 9 indicates that almost the same pattern of strength in the performance of the different corrugated core geometry can be seen, with rectangular having the highest strength, followed by trapezoidal and circular being close second and third, and lastly, triangular having the least load-carrying capacity. What is different, however, is that the amount of load the panel can carry has significantly increased.

Table 9.Summary of data under flatwise compression for foam-filled samples

Core Geometry	Weight [g]	Max Compression Force [kN]	Energy Absorbed [N.m]	Energy Absorption to weight ratio	Max Compression to Weight Ratio
Triangular	170.7	47.84	94.88	0.556	0.280
Trapezoidal	177.3	64.88	43.49	0.245	0.366
Rectangular	192.5	76.79	91.82	0.477	0.399
Circular	176.6	62.48	63.92	0.362	0.354

4.4 Effects of Foam infill on Bending strength

Lastly, the four foam-filled samples with different core geometries were tested under three-point bending, and the samples before and after failure are shown in Figure 4.7. Similar to the hollow samples, the triangular, trapezoidal, and circular panels show localized failure, while the rectangular panel shows global deformation. Buckling failure of the samples is accompanied by other forms of failure mechanisms such as adhesive shear, core cracking, and densification. In addition, dependant on the location of the top fixture and due to its rotational degree of freedom, sometimes core buckling was replaced by face sheet wrinkling.

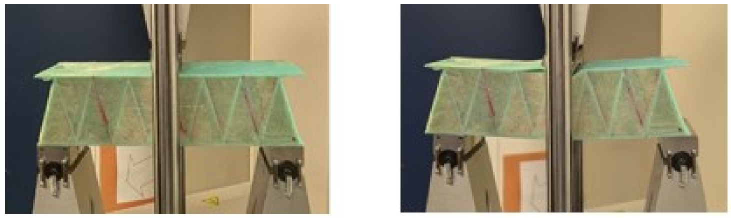

Triangular Corrugated Core with PET Foam Before and After Failure

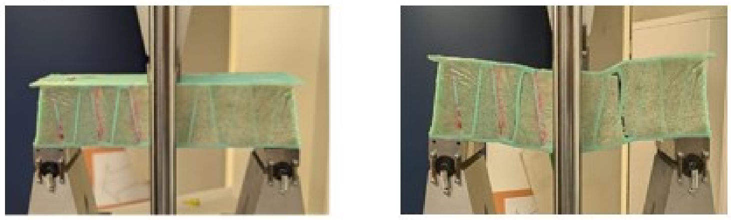

Trapezoidal Corrugated Core with PET Foam Before and After Failure

Rectangular Corrugated Core with PET Foam Before and After Failure

Circular Corrugated Core with PET Foam Before and After Failure

Figure 4.7. Corrugated core samples with PET foam infill under three-point bending load

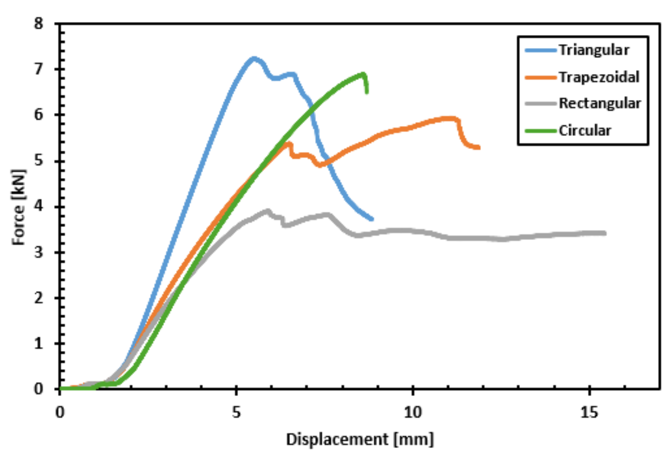

Figure 4.8. Force-displacement curves of the corrugated core panels
under three-point bending load

The force-displacement graph of the foam-filled corrugated core samples is shown in Figure 4.8. Similar to the bending of the hollow core, the graphs start with a linear elastic region followed by plastic deformation and buckling. As the load increases, the panels experience shear failure of the adhesive that is localized within the center of the samples. As the middle core buckles, the foam cell walls are crushed, and the densification results in a small plateau within the graph. In contrast to the hollow panels, where only the three middle corrugated channels experience buckling failure due to the energy distribution capabilities of the PET foam, the energy is slowly distributed to the outer cores as the central corrugated walls fail.

In the case of the circular panel, as soon as localized buckling of the central channel began, the bottom skin experienced fracture failure, creating a sudden drop in the load. It is important to note that the failure was due to stress concentration attributed to manufacturing irregularities. The second bending test performed on the circular core exhibited different failure mechanisms with similar compressive load. Lastly, the rectangular panel underwent global buckling of the structure. As the panel experienced more and more deformation, shear failure of the adhesive could be seen at the corners, causing a small, sudden drop in the force. As indicated in the summary of data seen in Table 10, the triangular has the highest flexural load-carrying capacity, followed by circular, trapezoidal, and rectangular.

Table 10.Summary of data under three-point bending for foam-filled samples

Core Geometry	Weight [g]	Maximum Force [kN]	Energy Absorbed [N.m]	Energy Absorption to Weight Ratio	Max Force to Weight Ratio
Triangular	257.1	7.24	15.43	0.060	0.028
Trapezoidal	278.8	5.94	15.47	0.055	0.021
Rectangular	292.8	3.90	10.54	0.036	0.013
Circular	274.8	6.89	27.66	0.101	0.025

4.5 Failure Mechanisms

Failure mechanisms are the different ways a material or component can fail under specific conditions. These mechanisms depend on the material, loading condition, and environmental factors. It is essential to investigate the failure mechanisms after testing; this can help understand material behavior, manufacturing issues, failure progression, and the weak points in the design or the material [74,75]. This section investigates the failure modes of the samples under compression and bending.

The different types of failure observed in the corrugated core and skins include buckling failure of the core, fracture of the core, cracking of the core, delamination of the core, fracture of the face sheet, and wrinkling of the face sheet. Each failure mode can be related to the material, loading condition, manufacturing method, and geometrical design. PLA material behaves elastically under low strain, exhibits some plastic deformation at higher stresses, and is considered brittle as it typically fractures after small deformations. As a result, the corrugated core and the skin of the panels experienced a fracture of the core and the face sheet after buckling. The layered nature of the samples from 3D printing triggered delamination of the core during buckling. Similarly, the voids resulting from the manufacturing process create stress concentration areas, leading to cracking within the core. Lastly, localized high stresses resulting from uneven loading can lead to wrinkles of the face sheet. This failure can indicate insufficient stiffness of the skin due to the choice of material or thickness as well as weak adhesion bonding. A schematic of each failure, along with pictures from the experimental samples, can be seen in Figure 4.9.

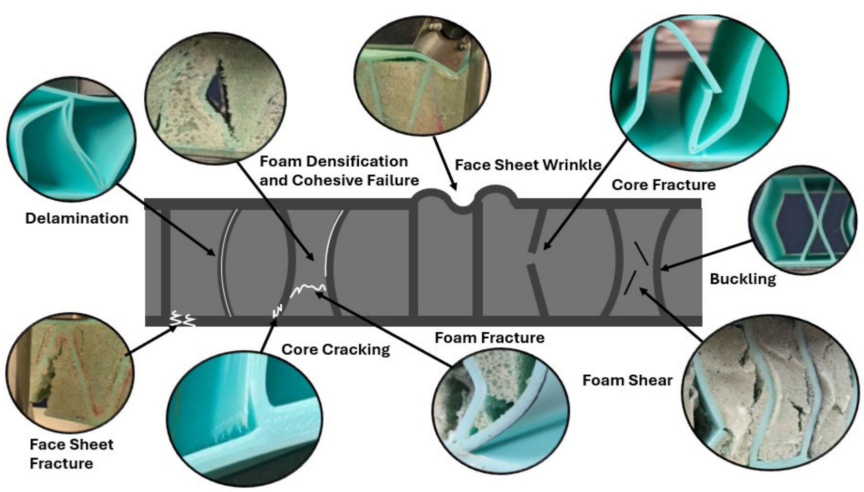

Figure 4.9. Failure mechanisms observed in corrugated core samples with and without foam

The types of failure detected within the foam under compression and bending include shear failure, fracture failure, densification, and cell collapse. As the shear force at the interface between the foam and cell wall increases, the high strength of the adhesive transfers the load to the foam, leading to shear failure. During buckling of the core, the foam cell walls collapse due to the increased pressure, causing the foam to compact in some areas, a process referred to as densification. Fracture failure of the foam occurs when the material is under an excessive amount of stress. This can be due to high stress concentration areas or excessive deformation during buckling of the foam, creating localized high stress-strain areas.

Lastly, some mechanical failures observed during testing can be related to the adhesive. The only types of failure identified related to the adhesive used to join the PET foam with the corrugated core walls were shear failure and cohesive substrate failure. During the plastic deformation of the samples, as the corrugated core starts to buckle, the increase in shear stress causes the adhesive to fail along the bond. After the corrugated wall separated from the foam was inspected, it was observed that the foam substrate fractured along the adhesion area, and the bonding did not fail. This shows that the adhesive is strong and capable of transferring the load efficiently and that the assembly process was done well.

After identifying the failure mechanisms and their underlying causes, changes can be made to improve the panels. Since the loading condition and material cannot be changed, the focus will be on the manufacturing process and the geometrical design. Although delamination of the core results from the nature of the Fused filament fabrication process, the interlayer bonding can be improved by adding a heated chamber. Increasing the temperature of the environment will keep the deposited layer malleable as the next layer is deposited, creating a better adhesion between the layers. In addition to a heated chamber, the print parameters, such as print speed, can be adjusted to decrease the number of irregularities and voids resulting from the manufacturing process. Doing so will reduce stress concentration areas and cracking failure. By analyzing the failure mechanisms that were not consistently observed across all samples, a comparative study is conducted to assess the stress levels in each panel.

For example, shear failure of the foam core was predominantly found in rectangular core samples, indicating that shear stress is higher in these panels due to the stress accumulation on the flat surfaces of the core. Increasing the core thickness can be a practical approach to reduce shear stress within the panel, as this would enhance stiffness. These factors can play a significant role in the future optimization of the panels.

4.6 Verification

The results obtained from the numerical model can provide a more in-depth understanding of the performance of the different core geometries under compressive and bending loads. Finite element analysis can demonstrate details that may be difficult to obtain through experimental testing, including stress-strain distribution and microscopic behavior, such as stress concentration. Figures 4.10-4.19 show the results obtained from the models, including the stress distribution and the force-displacement curves of the compression and bending samples. The distribution of mises stress can assist in determining areas of yield and stress concentration to understand the reaction of the panels under compressive and flexural loads and modify the design to improve functionality and structural integrity.

4.6.1 Compression

The compression models created on ABAQUS consist of the corrugated panel sample and two circular plate fixtures. The boundary conditions applied to the fixtures keep the bottom plate stationary with no degrees of freedom, and the top fixture is only allowed to move in the y direction. The compressive tests were performed by assigning a displacement to the top fixture and recording the reaction force. To understand the change in stress distribution throughout the test, multiple frames were captured for each sample. The captured frames start with the sample under no displacement and end at 1.5 mm displacement. Examining the behavior of each geometry offers important insights into their performance and key characteristics, as demonstrated below.

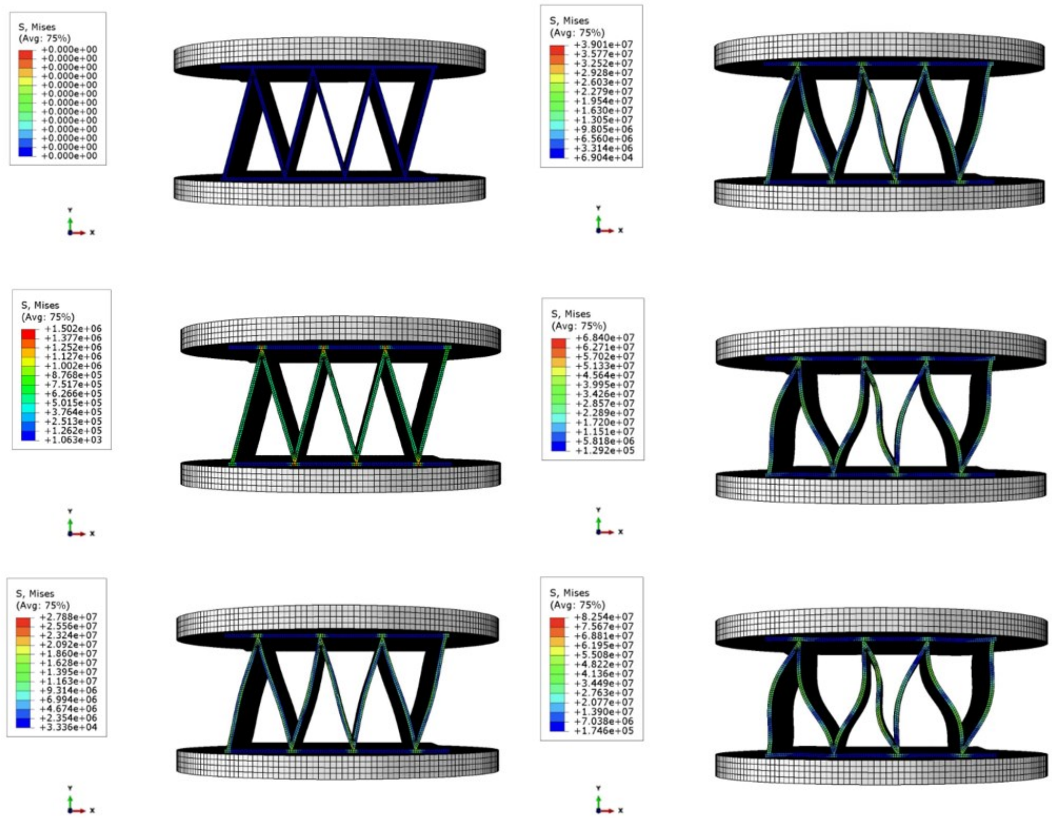

Figure 4.10. FEM showing stress distribution of triangular core panel under various compressive displacement

Triangular- When the triangular corrugated core panel is subjected to displacement, the stress becomes concentrated at the peaks and valleys of the core—specifically where it connects to the top and bottom skins. Once the core begins to buckle, the stress in those areas decreases due to the load distribution. When buckling occurs, the core can no longer sustain additional load through its original, pre-buckled structural configuration. out-of-plane deformations, which allow the structure to dissipate energy and carry loads through a combination of bending and membrane forces rather than pure compression. After initial buckling, the structure undergoes additional deformation that leads to additional forms of failure. In the case of the numerical study, post-buckling damage was not characterized. Lastly, the triangular core buckled in mode 1 due to its higher localized stress concentrations making it inherently prone to localized instability.

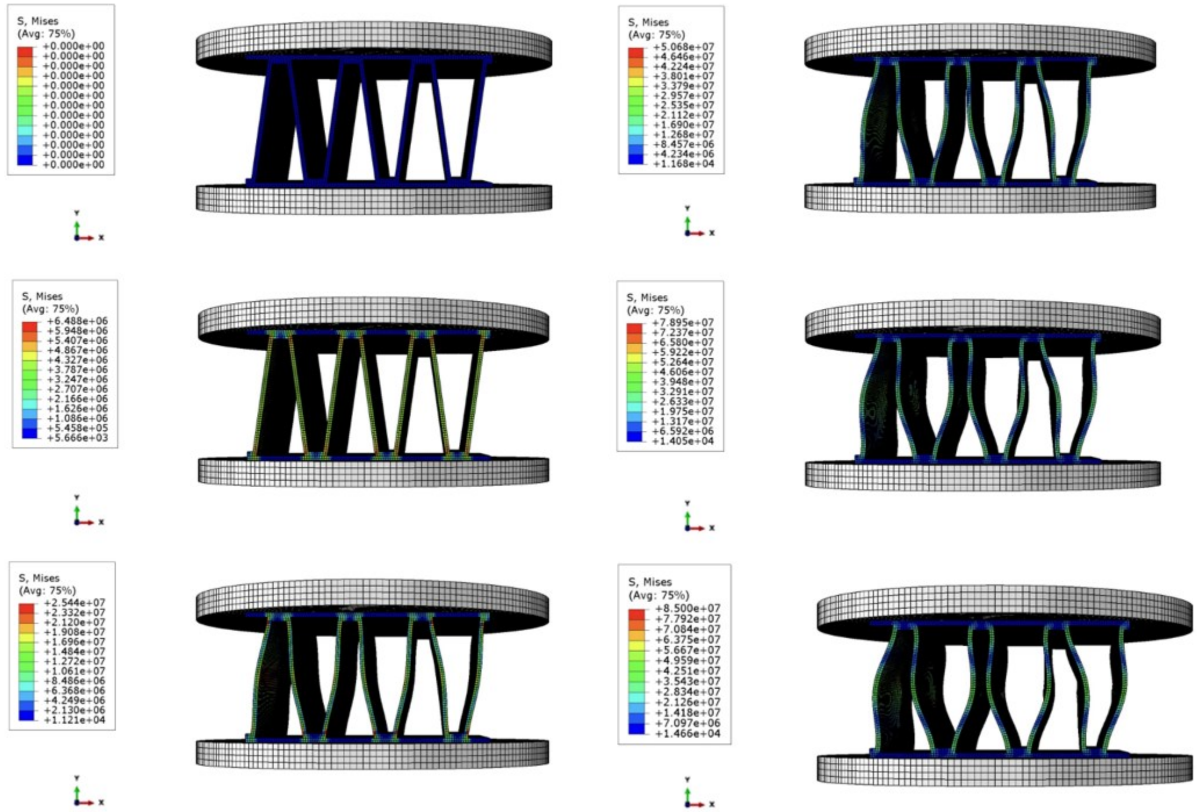

Figure 4.11. FEM showing stress distribution of trapezoidal core panel under various compressive displacement

Trapezoidal- When the trapezoidal corrugated core panel is subjected to displacement, stress concentrates at the joints where the inclined walls of the core meet the horizontal sections. This occurs because these areas have a larger cross-sectional area connecting the core to the skins. After the core buckles, the load is redistributed throughout the structure, reducing the stress that was previously concentrated in specific areas. After buckling, the structure deforms until it experiences other failure modes. It is important to note that, in the model, the corrugated core and the skins are assumed to have perfect contact, which may not be true in real life. In experiments, stresses are also expected at the connections between the core and the skins. The trapezoidal core has relatively horizontal walls, which help distribute stress more evenly. As a result, it naturally tends to buckle in global modes. Without the manufacturing imperfections typically found in real-world structures, the numerical model initially showed mode 2 buckling. To better reflect real-world behavior, imperfections were added to the model, allowing it to buckle in mode 1 instead.

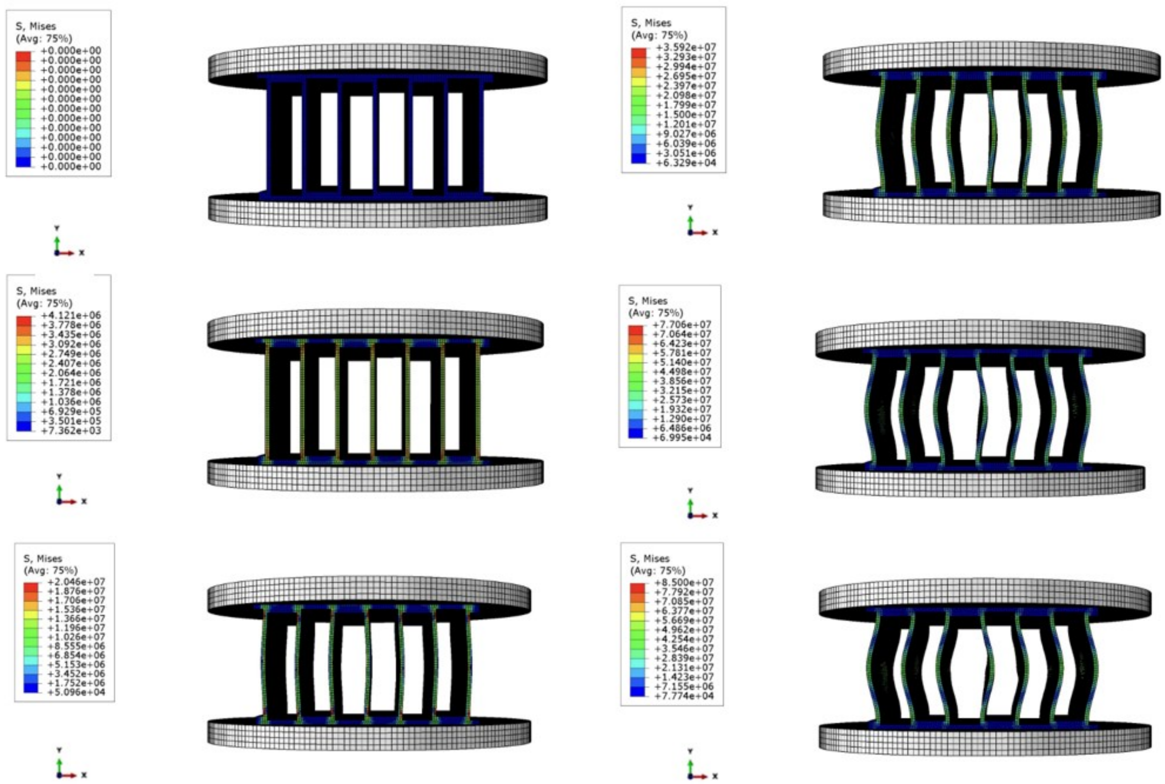

Figure 4.12. FEM showing stress distribution of rectangular core panel under various compressive displacement

Rectangular- When the rectangular corrugated core panel is subjected to displacement, stress is concentrated at the connection between the vertical walls of the core and the horizontal section of the core. When the critical load is reached, the structure can no longer maintain its equilibrium and starts to buckle. After buckling, the localized stresses are redistributed throughout the core, spreading across the structure and reducing the stress concentration in specific areas. Similar to the trapezoidal core, the stable geometry of the rectangular core caused the model to initially buckle in mode 2. Imperfections were introduced to trigger mode 1 buckling, which is necessary to better simulate real-world conditions. Without imperfections, higher buckling modes would occur at higher loads, leading to results that do not accurately reflect how the structure would behave in practice. Imperfections were added to the core to prevent inward buckling, which helps the model better match experimental results. This also stops the structure from re-stabilizing when the two buckled walls press against each other, preventing further deformation.

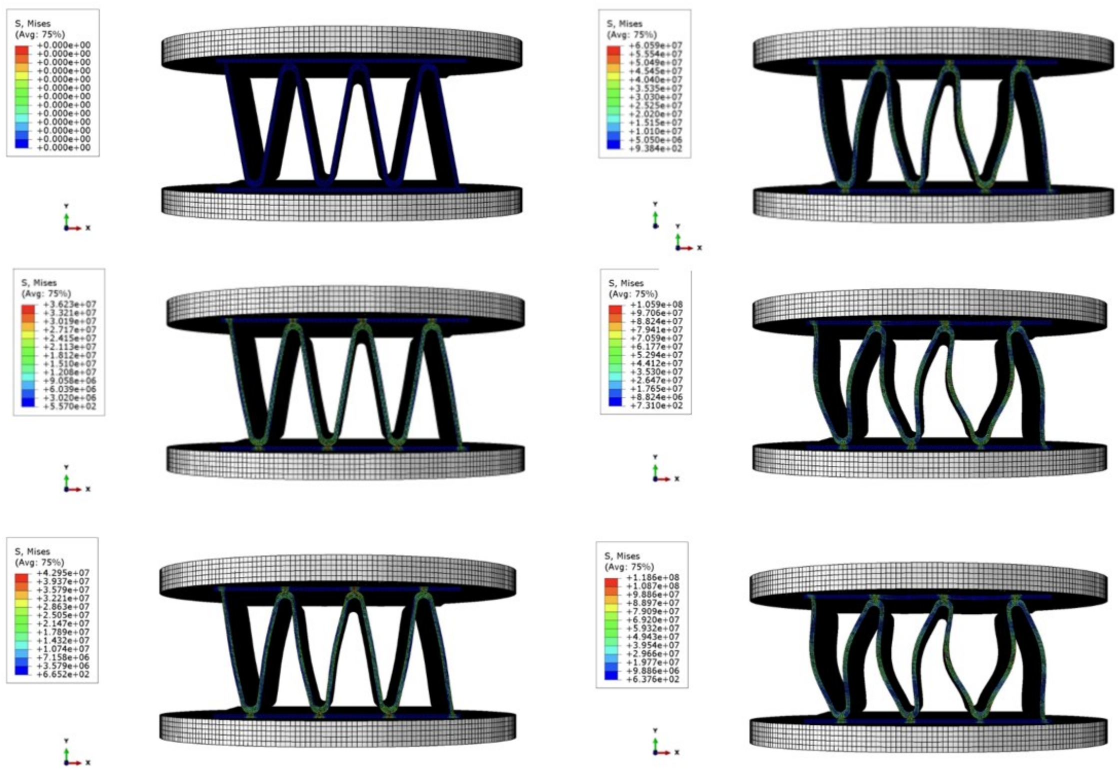

Figure 4.13. FEM showing stress distribution of circular core panel under various compressive displacement

Circular- When the circular corrugated core panel is subjected to displacement, stress is concentrated at the joint between the core and the top and bottom skins. As the critical load is reached, the core begins to buckle, distributing the load through the structure. This buckling deformation continues until another mode of failure is reached. Interestingly, in other cases, the maximum stress at a 1.5 mm displacement was typically found at the mid-span of the wall, on the side where it was under tension. However, in the case of the circular core, the highest stress after buckling occurs at the joint between the core and the skins. This suggests that the critical area in the design is the joint, as it has a small contact surface area.

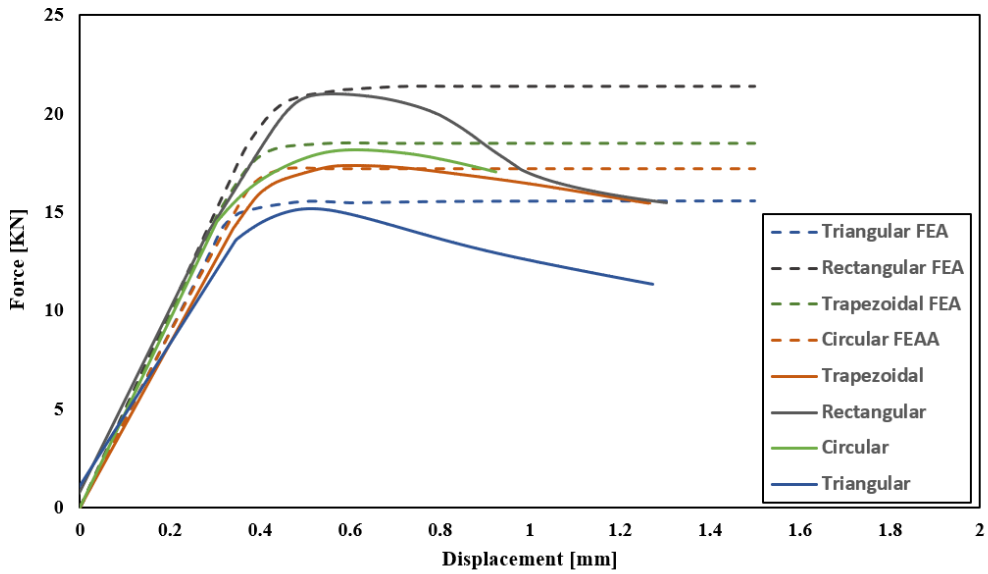

Figure 4.14. Force-displacement curves obtained from FEM of the corrugated panels under flatwise compression

The force-displacement curves obtained from the finite element modeling can be seen in Figure 4.14. Much like the experiment, the curves include a linear-elastic region followed by plastic deformation and buckling of the core. However, after buckling, the force remains constant because the various types of damage are not characterized in the analysis. The finite element analysis results show that in ideal conditions, the rectangular corrugated core panel is able to withstand the most amount of compression load followed by trapezoidal, circular, and triangular. The results are similar to the experimental, apart from trapezoidal and circular. During the experimental testing, the performance of trapezoidal and corrugated cores was close enough that in two of the tests, the circular was slightly better, while in one test, the trapezoidal was better. The maximum compressive load capacity before buckling the panels was found to have a 5-6% deviation from the experimental, which is within the acceptable range.

4.6.2 Three-point bending

The three-point bending models created on ABAQUS consist of corrugated core samples and three supports. The boundary conditions applied to the fixtures keep the two supports at the bottom stationary with no degrees of freedom, and the top support is only allowed to move in the y direction. The flexural tests were performed by assigning a displacement to the top fixture and recording the reaction force. Multiple frames were captured for each sample to understand the change in stress distribution throughout the test. The captured frames start with the sample under no displacement and end at 20 mm displacement for the rectangular sample and 10 mm for the other three samples. Examining the behavior of each geometry offers important insights into their performance and key characteristics, as demonstrated below.

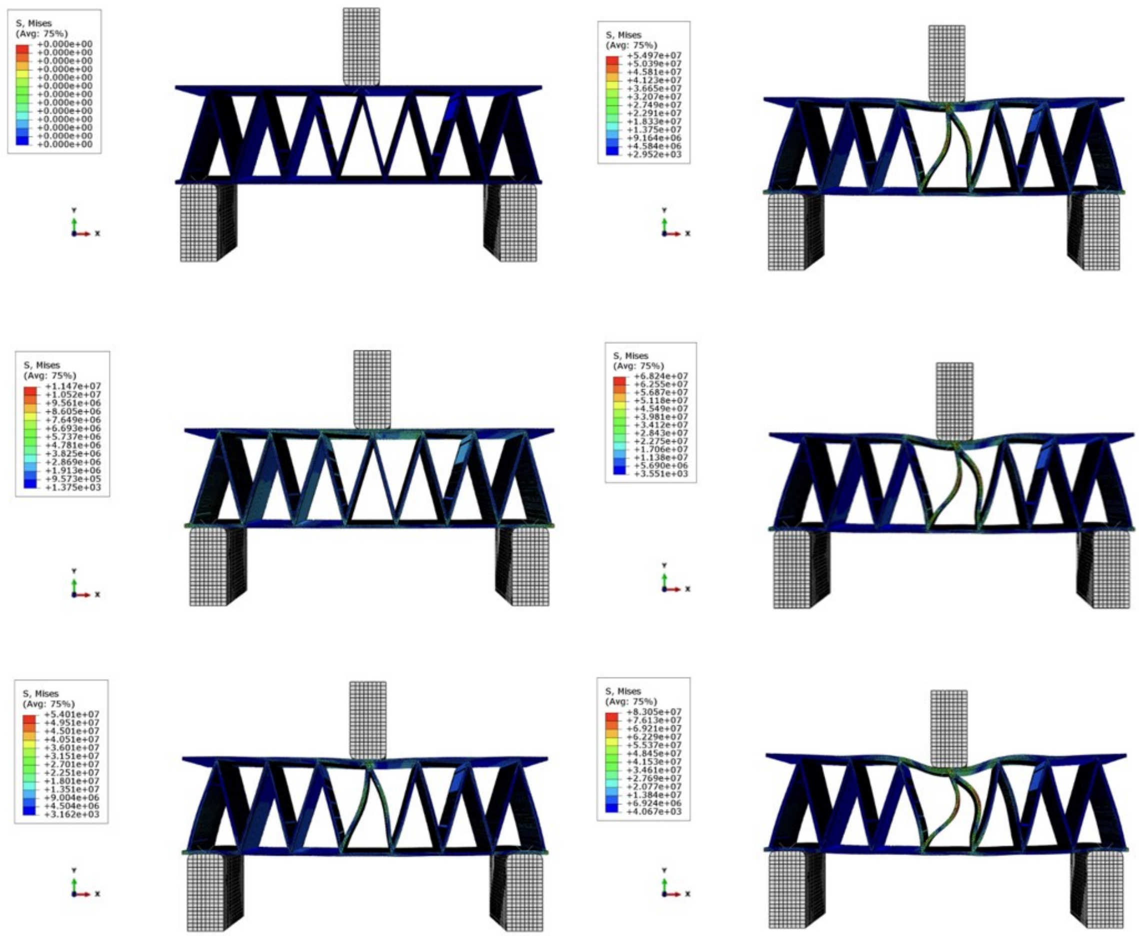

Figure 4.15. FEM showing stress distribution of triangular core panel under various flexural displacement

Triangular- when the triangular corrugated core sample is subjected to displacement, the stress is concentrated under the supports and the joint locations where the core is bonded to the skins. It was observed that when the load reached its critical value, the central core beneath the top support buckled, causing the skin to deform along with it. As the displacement increased, the unit cell at the midspan of the sample continued to deform progressively. Interestingly, there was very little load redistribution to the rest of the core or the skin after deformation. This highlights the importance of the force application point in corrugated core sandwich panels and the ability of the core to distribute the load. Further investigation using finite element models could provide deeper insights into this behavior.

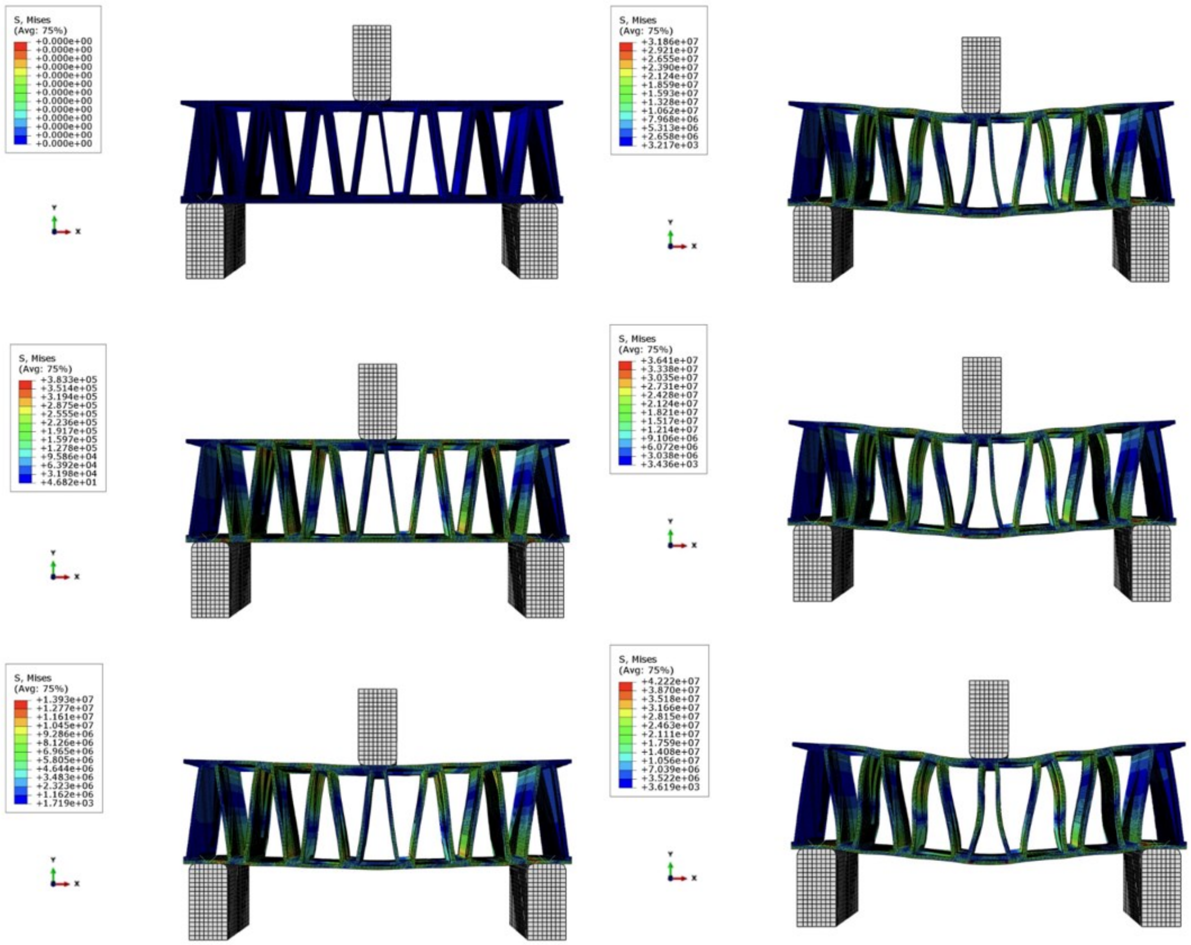

Figure 4.16. FEM showing stress distribution of trapezoidal core panel under various flexural displacement

Trapezoidal- When the trapezoidal corrugated core sample is subjected to displacement, the stress is primarily distributed across the two channels on the right and the two channels on the left of the top support, where the load is applied. Within these channels, stress concentrations are higher at the top and bottom of the inclined walls, where the core connects to the skin. As the load approaches the critical value, the five central channels undergo global buckling, demonstrating effective load distribution in this geometry. With further displacement, the core continues to deform, and the skins begin to wrinkle. This occurs because the horizontal sections of the core are thicker and, therefore, stronger. As a result, areas with thinner sections deform more easily, while the thicker sections remain flat. The two outermost channels experience the least amount of stress, highlighting the load distribution pattern in the structure.

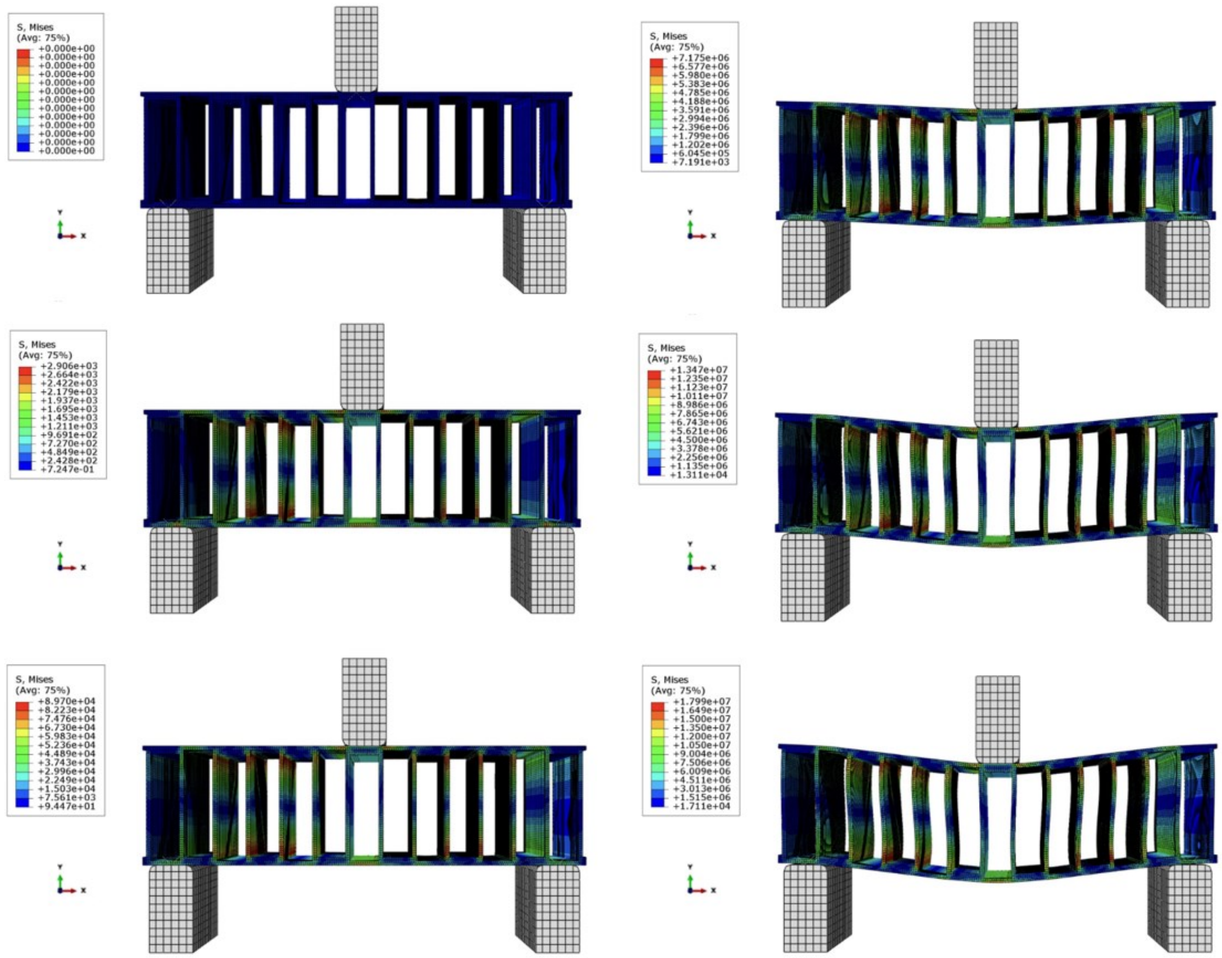

Figure 4.17. FEM showing stress distribution of rectangular core panel under various flexural displacement

Rectangular- When the rectangular corrugated core panel is subjected to displacement, the stress is distributed across the two channels on the right and the two channels on the left. Within these channels, the highest stress is concentrated at the top and bottom of the vertical walls, where the core connects to the top and bottom skins. As the displacement increases, the load increases without causing buckling. This leads to higher stresses that propagate to even the last corrugated channels at each end. Once the critical load is reached, the structure undergoes global buckling. Since the corrugated panels do not have localized buckling, the stress remains concentrated within them, continuously increasing until the structure can no longer support the load and ultimately fail. Localized buckling is usually preferred because it leads to more controlled and predictable failure, while global buckling can cause a sudden and catastrophic collapse of the entire structure.

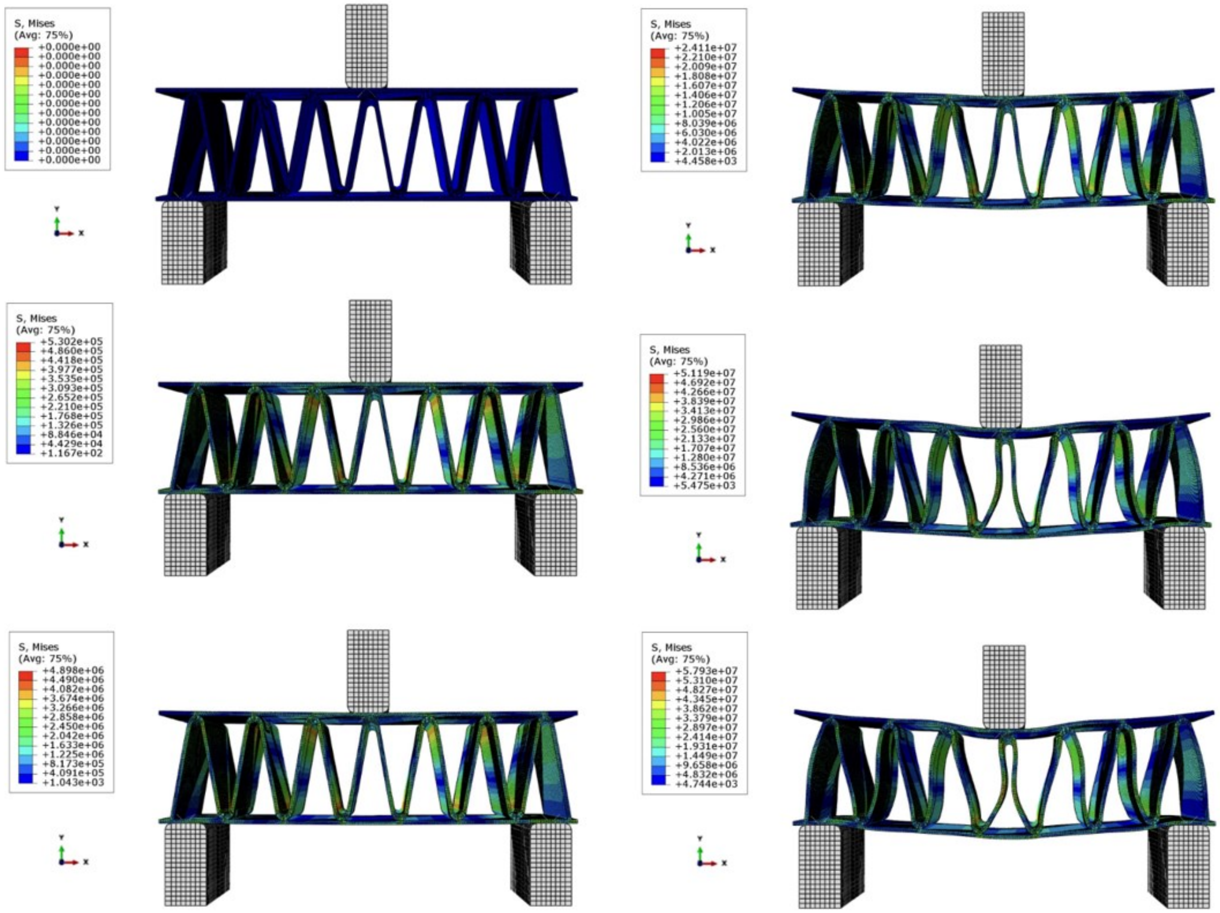

Figure 4.18. FEM showing stress distribution of circular core panel under various flexural displacement

Circular- When the circular corrugated core panel is subjected to displacement, the stress is spread throughout the entire core. The areas of highest stress concentration occur at the peaks and valleys of the core, where it connects to the skin. This is due to the small contact surface, which limits how the load is transferred. When the load reaches the critical value, the entire core experiences localized buckling. Although this core shows excellent load distribution, the small contact area between the core and the skin remains a key weakness.

According to the finite element model, the triangular core, although resistant to buckling, does not distribute the load effectively under three-point bending. Within the trapezoidal and circular samples, the central core begins to buckle, and the stress is distributed to the channels on each side one by one. Unlike the other three geometries, the walls of the rectangular core begin to buckle at the same time, but then the structure experiences global deformation. Through the stress distribution visualization tool, some of the assumptions made from the experimental results were found to be flawed, while other details remained hidden.

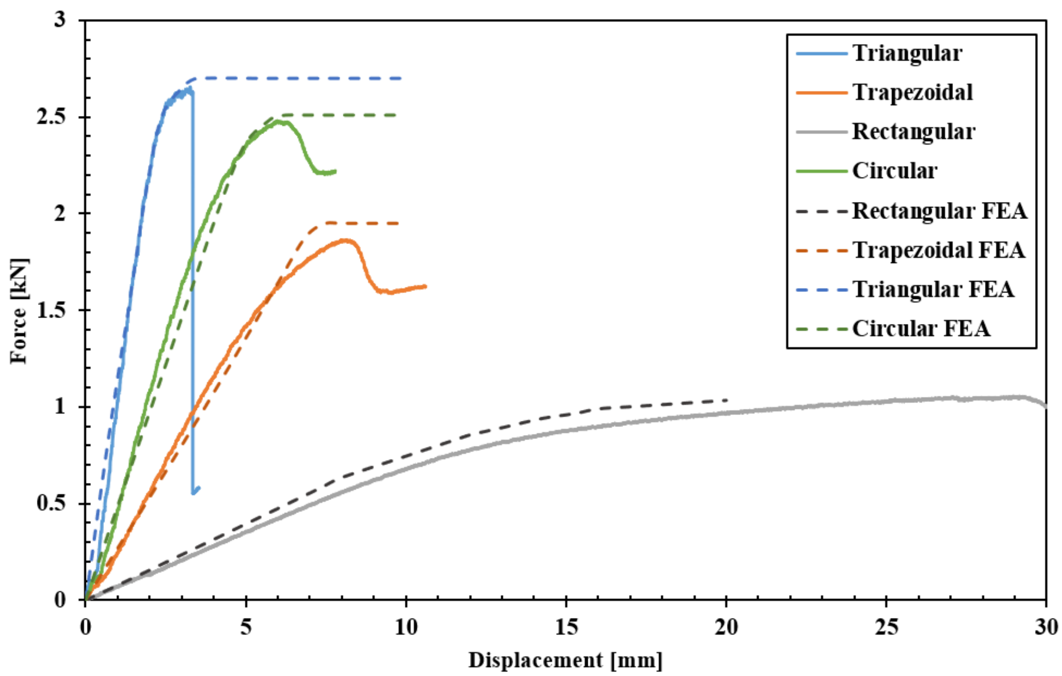

Figure 4.19. Force-displacement curves obtained from FEM of the corrugated core panels under three-point bending

The force-displacement graph obtained from FEA closely matched the experimental results for the triangular and circular cores. The results for the rectangular and trapezoidal panels exhibited a higher percentage difference, which can be attributed to the presence of sharp corners where the 3D printing process is more susceptible to void formation. Since the core buckling is considered a failure and the purpose of the models is not to investigate the failure mechanism, no damage was defined. As a result, the graphs only represent the elastic and plastic regions up to buckling failure.

4.7 The Effect of Load Location in Three-Point Bending

The location of the supports and applied load in the three-point bending test is important in corrugated core panels because it significantly influences the stress distribution, failure modes, and load-carrying capacity of the structure. Loading applied directly on top of a peak or in between two peaks can affect bending behavior. The point of load application creates stress concentration at the applied location. If the load is applied at a structural weak point the panel can experience faster failure. The finite element models provide a flexible, cost-effective, and time-saving tool to study these scenarios without the need for sample manufacturing and extensive experimental testing setup.

The load-carrying capacity of a corrugated core sandwich panel depends significantly on where the load is applied. If the load is applied at the peak, the load has a direct path and can enhance load distribution. Furthermore, the structure is inherently better supported at the peak, making it a strong point that can resist deformation during loading. The disadvantage of loading at the peak is that the applied load can create stress concentration at the peak that can lead to localized buckling failure. If the load is applied between two peaks, the skin can deform if there are no supports directly underneath the fixture applying the load. Also, valleys are typically less structurally supported, leading to lower strength in that region. Although applying the load at the peak is expected to be more favorable for maximizing load carrying capacity of the panels, the exact performance will depend on the specific geometry and material. FEA models were used to study how the location of the load affects the flexural performance of sandwich panels with different core geometries. To ensure consistency, all settings were kept constant, and the panels were rotated 180 degrees about the x-axis to keep the load applied at the center of the panel.

The results indicate that the panels can carry less load when the load is applied between two peaks compared to when it is applied directly on top of a peak. This effect is more noticeable in panels with triangular, trapezoidal, and circular core geometries than in those with rectangular cores. The rectangular symmetry and uniform structure of the rectangular core allow the load to distribute more evenly throughout the core, making the location of the load less critical.

When the fixture provides no direct support from the core, the applied load is transferred to the skin, which acts as a buffer. This buffering effect can reduce the overall stress distributed within the core by partially absorbing and redistributing the applied load. However, this also means that the skin bears a greater portion of the stress, making it more susceptible to localized deformation or failure. Overall, applying the load to the skin instead of directly on the core can alter the load distribution and failure mechanisms, potentially reducing the overall load-carrying capacity and introducing new points of weakness in the structure.

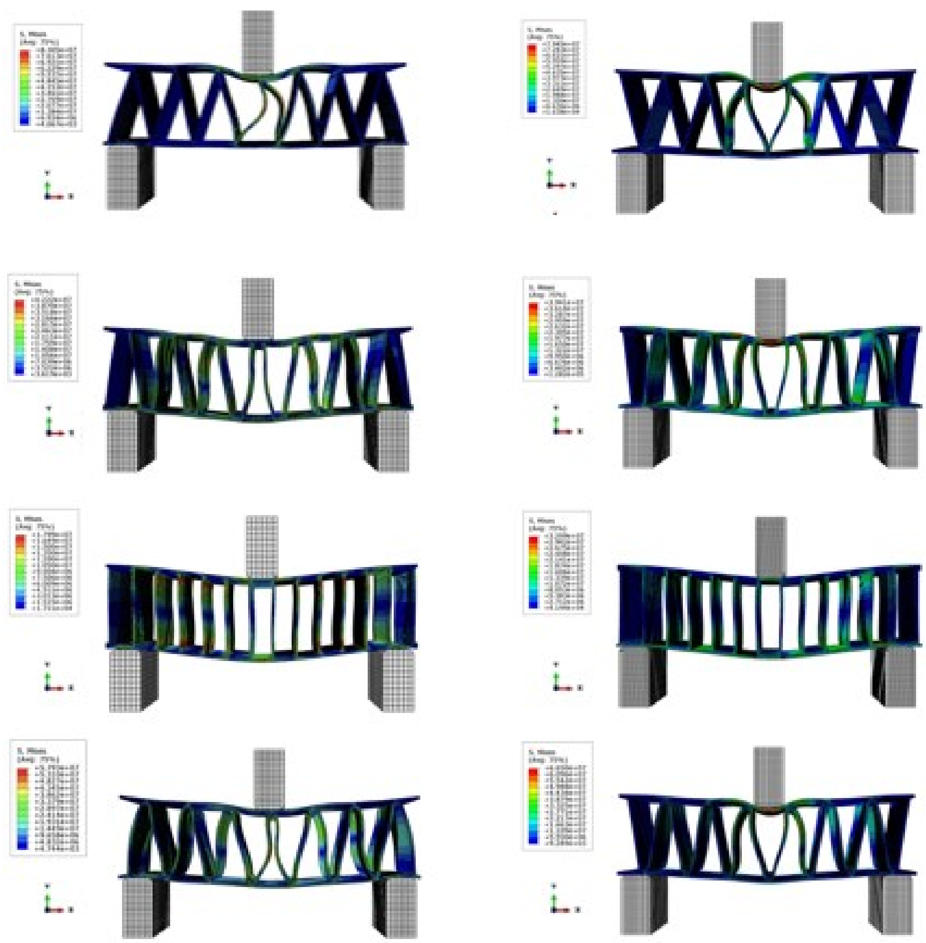

Figure 4.20. FEM showing stress distribution of corrugated core panels under flexural displacement

The graph is shown in Figure presents the force-displacement curves of the panels with various loading locations.

The flexural load-carrying capacity of the triangular core decreased by 28.5%, while the trapezoidal and circular cores saw reductions of 19.75% and 22.2%, respectively. In contrast, the rectangular core showed a much smaller decrease of less than 10%.

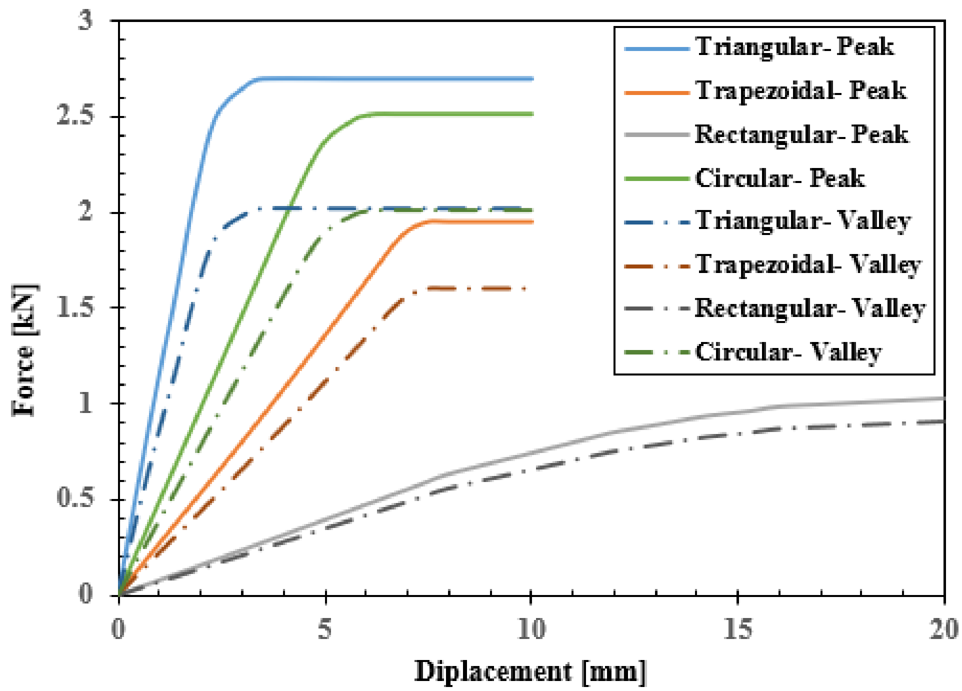

Figure 4.21. Force-displacement curves obtained from FEM under flexural load in different locations

One of the core panels was tested by applying the load at the valley to compare the results with the simulation predictions. As shown in Figure , the experimental results indicate that the skin deformed under the load, after which the force was transferred to the two nearest corrugated unit cells, causing them to buckle. The compressive load capacity in this setup was lower than when the load was applied at the peak. These findings are consistent with the results from the finite element models.

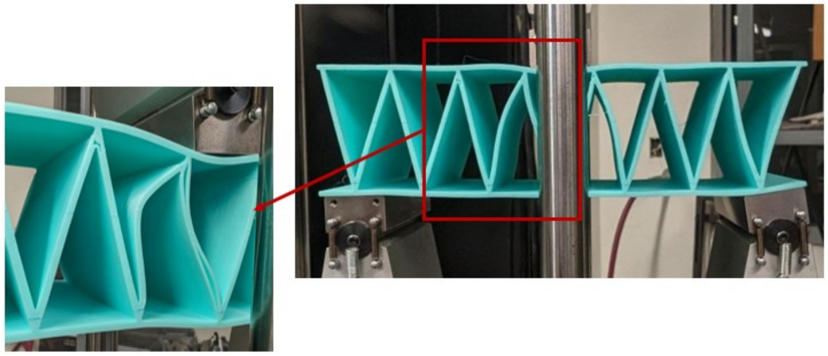

Figure 4.22. Triangular corrugated core sample without PET foam infill under three-point bending load applied to the valley

4.8 Optimization case studies

The core geometries investigated in this research have not undergone optimization. A comprehensive optimization process would require an extensive analysis of various geometrical parameters and their influence on structural performance under different loading conditions. Due to the scope constraints of this study, a full optimization was not feasible. However, select case studies were conducted to demonstrate how the finite element analysis (FEA) models developed in this research can be utilized to guide future optimization efforts.

4.8.1 The effect of cell wall thickness on compressive performance

The validated finite element models can significantly aid in optimizing the design of corrugated core panels by refining key structural parameters such as core wall thickness, skin thickness, corrugation angle, radii, and the number of corrugations. To demonstrate this capability, two factors were selected and analyzed for one of the corrugated core panels. The circular and trapezoidal cores showed the most promise among the tested core geometries. In contrast, the rectangular and triangular cores, while performing well in either compression or bending, were weaker under other loading conditions. This section demonstrates how the cell wall thickness of the circular core affects its compressive load-carrying capacity.

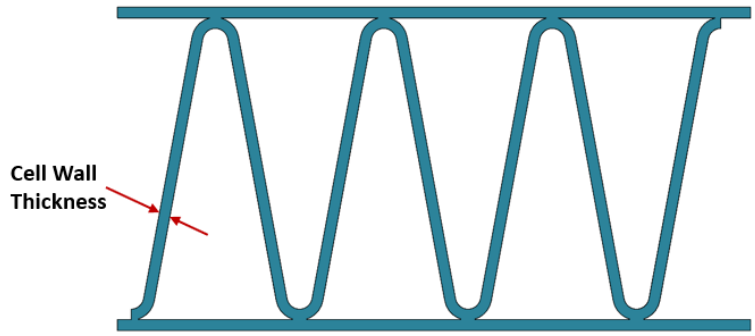

Figure 4.23. Geometry of circular corrugated core sandwich panel with variable cell wall thickness

The initial core design featured a wall thickness of 1.78 mm. To investigate the influence of wall thickness on mechanical performance, this parameter was systematically varied by both decreasing and increasing the thickness in 25% increments. The original CAD model was developed using surface modeling techniques, which facilitated modifications to the wall thickness without altering the overall geometry. In this method, the core geometry is first defined by a line profile, and the desired thickness is subsequently applied symmetrically on both sides of the profile. To maintain consistency, the core height was adjusted accordingly to preserve an overall sandwich panel thickness of 2 inches. Additionally, the surface contact area between the core and the face sheets was held constant to ensure that any observed variations in mechanical performance could be attributed solely to changes in wall thickness, minimizing the influence of other variables.

Increasing the thickness of the cell wall is expected to have several impacts on its compressive performance, such as an increase in compressive strength, stiffness, increased weight, and failure mode transition. Thicker cell walls can bear more load before failure, leading to an increase in compressive strength as the load is distributed through a larger cross-sectional area, reducing local stress concentration. While mechanical performance improves, the weight of the panel increases. This trade-off may not be ideal in applications where weight is crucial. Depending on the extent of thickness increase, failure mode can shift from buckling to compressive failure mechanism. Buckling failure is associated with thin-walled structures.

Table 11. Summary of data of circular core under compression with thickness variation

Model Name	Weight [g]	Thickness [mm]	Maximum Load [kN]	Normalized Force [N/g]
Thickness 1	85	0.860	2.19	25.96
Thickness 2	94	1.075	4.85	51.82
Thickness 3	107	1.383	9.85	91.72
Thickness 4	125	1.778	17.20	137.58
Thickness 5	148	2.286	32.80	221.95
Thickness 6	171	2.857	70.05	409.90

Finite element analysis reveals that increasing the wall thickness by 25% leads to a 100% rise in load capacity, up to a thickness of approximately 2.2 mm, beyond which the increase becomes more pronounced. However, each 25% increase in thickness of the core also results in an increase in weight of 10-15%. Figures 4.24 and 4.25 represent the correlation between change in thickness with changes in compressive load capacity and weight of the panel.

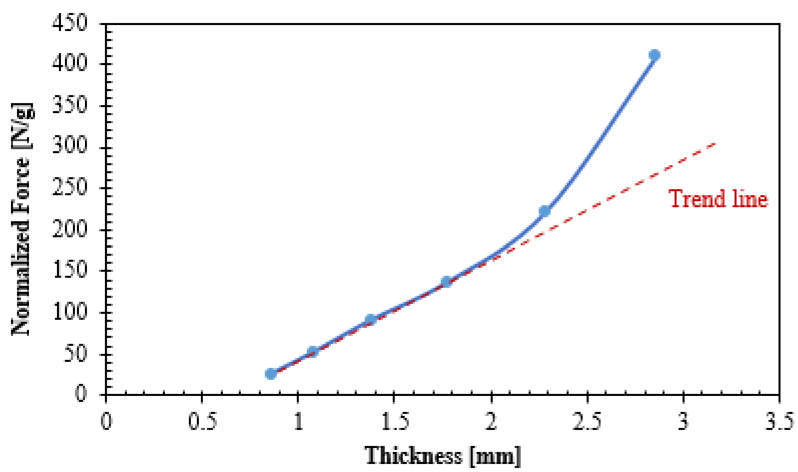

Figure 4.24. Maximum normalized compressive force vs. thickness obtained from FEM

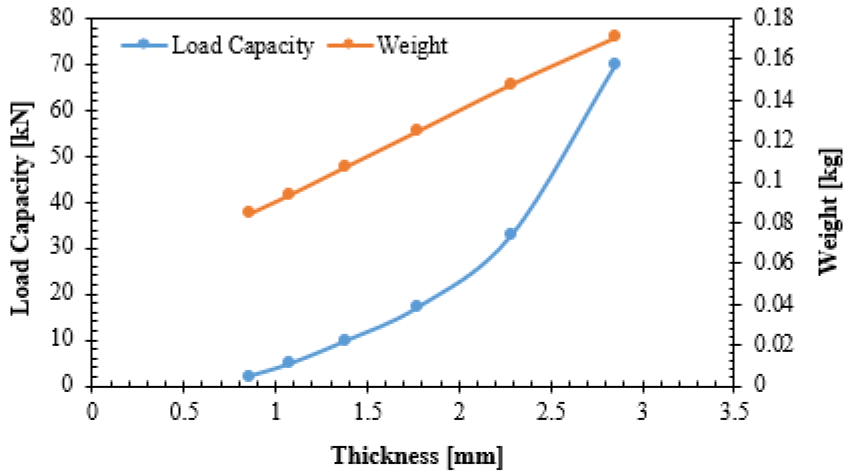

Figure 4.25. Maximum compressive force and weight vs. thickness curves obtained from FEM

Having identified the effect of wall thickness on the compression performance of the panel, it can be concluded that, depending on the application, increasing the thickness, provided weight is not a critical design constraint, can significantly enhance the strength of the panel. In the case of this study, the core cell wall thickness was not increased enough to lead to a change in the failure mechanism. Generally, buckling failure is preferred over compressive failure as it results in less immediate structural damage, offering more opportunity for controlled failure.

4.8.2 The effect of Angle on compressive performance

This section examines the influence of the corrugation angle of the circular core on its compressive load-carrying capacity. The initial core design featured a corrugation angle of 21 degrees. To evaluate the impact of this angle on compressive performance, the corrugation angle was systematically decreased and increased in 25% increments. Other geometric parameters, such as the radius of curvature and number of corrugations, were kept constant to isolate the effect of the corrugation angle on the results. It is important to note that as the corrugation angle increased, the panel length had to be adjusted to maintain a consistent number of corrugations. This adjustment resulted in larger face sheets, which, while not significantly affecting the compressive performance, did lead to a considerable increase in the weight of the sample.

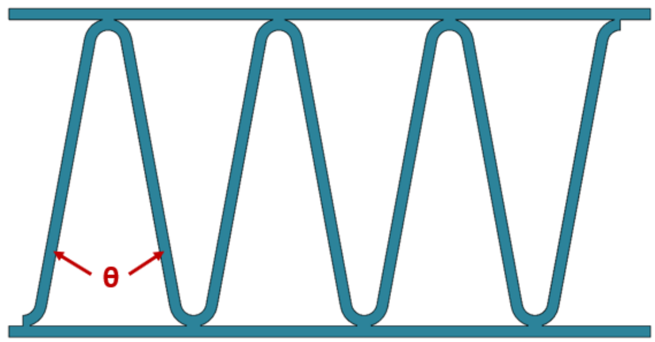

Figure 4.26. The geometry of circular corrugated core sandwich panel with variable angle

Increasing the corrugation angle in a circular structure can significantly affect its compressive performance by altering the load distribution, structural stiffness, and failure modes. A larger corrugation angle is expected to reduce the ability of the core to effectively distribute compressive loads. As the corrugations become flatter, the resistance of the panel to compression diminishes, leading to an increased likelihood of buckling failure along the corrugated walls. In contrast, smaller corrugation angles result in a steeper, more tightly packed core, which enhances its ability to resist deformation under compression and improves overall structural performance. Although the general expected trend is understood, the FEA model provides a valuable tool for quantitatively assessing the impact of the corrugation angle on load capacity. It allows for a deeper analysis of whether this effect allows a linear relationship or exhibits a more complex behavior.

Table 12. Summary of data of circular core under compression with angle variation

Model Name	**Weight [g]**	***Angle*** °	**Maximum Load [kN]**	**Normalized Force**
Angle 1	119	16.8	18.53	155.21
Angle 2	125	21	17.04	136.33
Angle 3	130	26.25	15.17	116.76
Angle 4	144	32.81	14.31	99.15
Angle 5	152	41.02	13.63	89.36
Angle 6	169	51.25	13.60	80.57

Finite element analysis (FEA) demonstrates that increasing the corrugation angle by 25% results in a 10% decrease in load capacity up to an angle of 25 degrees, followed by a 5% decrease up to 40 degrees. Beyond this point, the load capacity reaches a plateau where it remains stable. Figures 4.27 and 4.28 represent the correlation between changes in thickness with changes in compressive load capacity and weight of the panel.

The analysis indicates that smaller corrugation angles typically result in higher strength. However, it is important to note that this increase in strength is accompanied by an increase in weight, as the number of corrugations was kept constant in the study. If the panel size is held constant instead, a larger corrugation angle would result in fewer unit cells, thereby reducing the overall weight. Additionally, a larger corrugation angle may enhance the manufacturability of the panel, particularly in processes such as molding and forming. Ultimately, the choice of corrugation angle must be carefully optimized, taking into account the specific performance requirements and manufacturing constraints of the application.

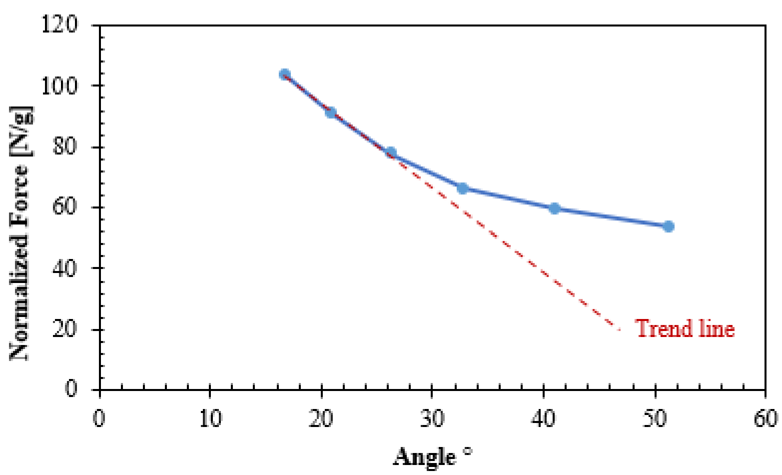

Figure 4.27. Maximum normalized compressive force vs. corrugation angle obtained from FEM

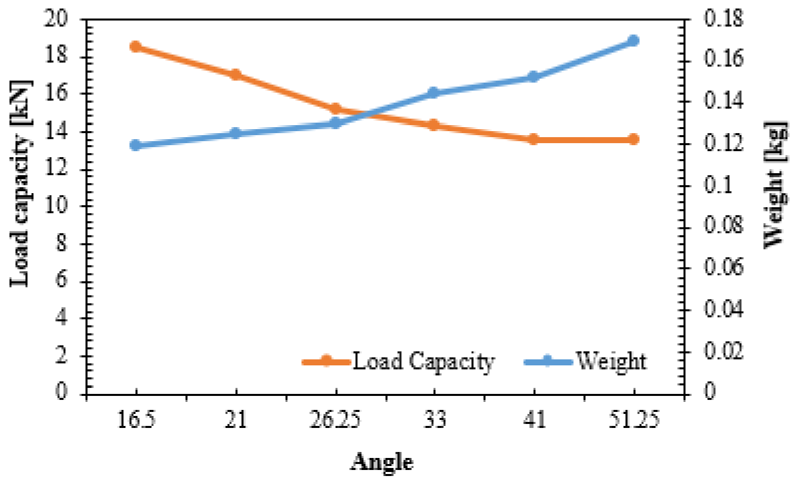

Figure 4.28. Maximum compressive force and weight vs. corrugation angle curves obtained from FEM

4.9 Comprehensive Analysis

The goal of this research is to support the development of a multifunctional corrugated core sandwich panel for use in the construction industry. To achieve this, various core geometries were analyzed and compared based on their performance under compression and bending loads. This section provides a detailed evaluation of each core geometry, highlighting their strengths and weaknesses using insights gathered from both experimental testing and finite element modeling.

The rectangular core demonstrated the highest compressive strength among the tested geometries. Its vertical walls create a direct load path, efficiently transferring compressive forces from the top skin to the bottom skin. This design promotes even load distribution preventing bending forces during compression. However, despite its excellent performance under compression, the rectangular core performed ineffectively under bending loads. The vertical supports are relatively short and stiff compared to the span of the structure. A longer span in the bending direction contributes to the global deformation mode, which dominates over local buckling. Although the rectangular core had a much lower flexural load capacity compared to the other three geometries, global bending deformation offers a more controlled, gradual response to loading.

The triangular core has weaker performance under compression but performs better under bending. The sharp angles of the triangular geometry create areas where stress concentrates. When compressed, this leads to local buckling or failure at those points. The angular design of the walls doesn't provide as direct a path for load transfer as other geometries, like the rectangular core. This was particularly evident in bending, where the load wasn’t distributed effectively through the core, causing localized buckling in the channels under the load. The lack of vertical support in the triangular core makes it weaker in compression, whereas the diagonal orientation of the walls provides better resistance to bending. While localized failure in the triangular core can result in more controlled damage and reduce the risk of a catastrophic collapse, it also leads to less energy absorption compared to other geometries.

The trapezoidal and circular corrugated cores demonstrated good compressive strength. However, the trapezoidal core tended to concentrate stress at the joints where the inclined walls connect to the skin. This design also introduced bending stresses in the walls, making them more prone to buckling. In contrast, the circular core experienced localized buckling at the peaks and valleys where it connects to the skins. Despite this, both cores showed effective load distribution and flexural performance, with the circular core performing better in bending. The smooth, curved design of the circular core allowed for a gradual transition of stress, reducing stress concentrations and improving its ability to handle bending loads more efficiently. Both circular and trapezoidal cores perform well in applications that require a combination of good compressive strength and bending strength.

The addition of foam infill helped distribute the load more evenly across the sandwich panels, increasing their resistance to compression and reducing the likelihood of local buckling or failure. The foam also supports the skins, ensuring their structural integrity under compression. In addition, the foam infill enhances the panel’s flexural strength and energy absorption capabilities. As the foam compresses and deforms, it dissipates energy, making the panel more resilient. The compressive strength of the panels increased by 200-345% with only a 32.5% increase in weight. Similarly, the flexural strength improved by 170-267% while the weight increased by an average of 40%. This significant increase in strength justifies the added weight.

In certain applications, such as construction, where weight is less critical than strength, the improved performance from the foam infill may make the weight increase worthwhile, ensuring the structure can handle necessary loads without additional reinforcement. Figures 4.29 and 4.30 illustrate force-displacement curves showing the significant difference in the compressive and bending performance of the panels with and without foam infill, as well as a bar chart representing the increase in weight vs. increase in load capacity of each core geometry.

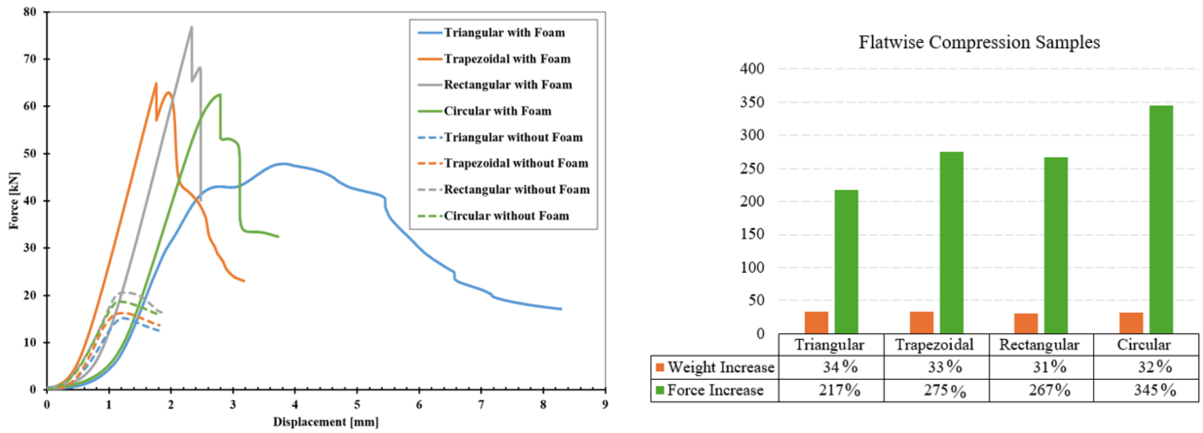

Figure 4.29. Force-displacement curves and bar chart of samples with and without PET foam infill under flatwise compression load

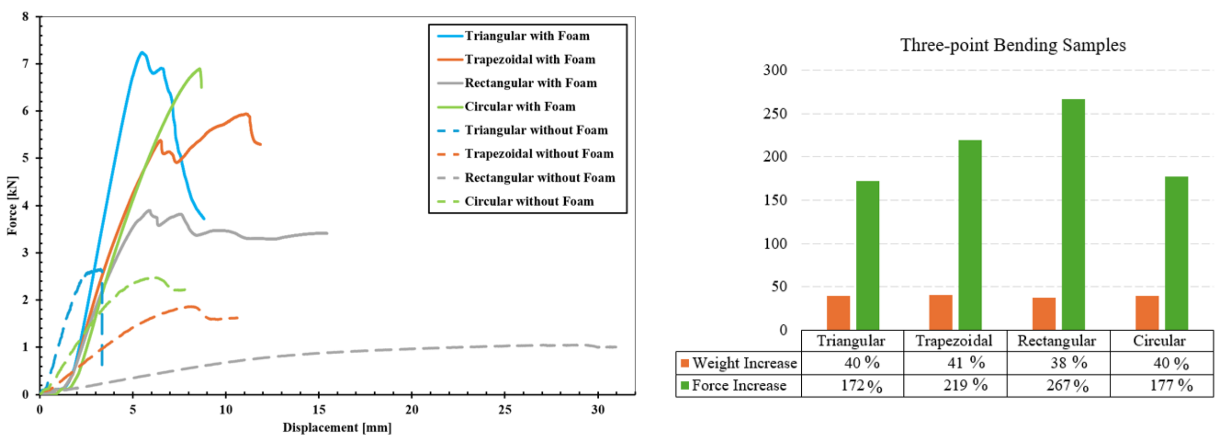

Figure 4.30. Force-displacement curves and bar chart of samples with and without PET foam infill under three-point bending load

Chapter 5: CONCLUSION, CONTRIBUTIONS, AND FUTURE WORKS

5.1 Contributions

This research extensively explored the performance of corrugated core sandwich panels with different core geometries, all manufactured using 3D printing. The panels, featuring triangular, trapezoidal, rectangular, and circular core geometries, were subjected to flatwise compression and three-point bending tests. The compressive capacity, flexural capacity, and energy absorption capabilities of the panels were compared. A finite element model was then used to validate the experimental data and provide deeper insight into the stress distribution of each core geometry.

Furthermore, the study investigated the impact of foam infill on the compressive and flexural strength of the panels.

The key findings from the experiments conducted are summarized as follows:

- **Flatwise Compression Test Results:** The rectangular core demonstrated the highest compressive strength, followed by the circular and trapezoidal cores, which exhibited nearly identical performance. The triangular core had the lowest compressive strength. All samples failed through mode 1 buckling.

- **Three-Point Bending Test Results:** The triangular core exhibited the highest flexural strength, followed by the circular, trapezoidal, and rectangular cores. All samples failed through mode 1 localized and global buckling except for the rectangular core, which failed through deformation failure of the structure.

- **Flatwise Compression Test with PET Foam Infill:** Panels with PET foam infill demonstrated an average 275% increase in compressive strength with only a 32.5% increase in total weight.

- **Three-Point Bending Test with PET Foam Infill:** The panels with PET foam infill also showed, on average, a 220% increase in flexural strength with just a 40% increase in total weight.

- **Numerical Modeling Verification:** All the models were verified using the experimental data and used to investigate the stress distribution within the panels under compression and bending.

- **Numerical Modeling Results:** Later, the finite element models were used to investigate the effect of load application location in three-point bending and to perform case studies investigating the effect of cell wall thickness and corrugation angle on the performance of the circular core under compression.

These findings provide valuable insights into the performance of corrugated core sandwich panels with varying geometries and foam infill, highlighting their potential for use in applications requiring high strength and energy absorption.

5.2 Future works

This research provides a solid foundation for future work and highlights areas that require further investigation, such as geometrical design optimization and industrial design/manufacturing case study. As shown in section 4.8, the finite element models created during this study can be used to investigate the effect of geometrical factors on the performance of the panels to further optimize the geometries. Factors such as the thickness of the skin, number of corrugations, radius, and more still need to be investigated in order to understand the potential of each geometry to create an optimum panel. Building on this study, more industrial materials can be explored. Specifically, the study does not address the properties of sandwich panels made from materials commonly used in construction, like various types of fiber-reinforced polymers (FRP), due to the rigid requirements of the manufacturing process. Multiple molds would have been needed to compare the performance of different core topologies using FRP materials, making the process inefficient. To address this, performance and design optimization were compared using 3D printing and PLA material. The Finite Element Analysis (FEA) models developed in this study can help examine the performance of different core geometries with alternative materials.

The primary goal of this research was to contribute to developing a multifunctional and sustainable panel. However, a complete industrial design and manufacturing study must continue this work. Initially, the panels' performance can be compared by incorporating the desired material into the FEA model. Once the functionality of the cores is confirmed, the next step will involve investigating the manufacturing process for each core. For efficient panel production, the design should be simple enough to be easily fabricated using existing technology, with minimal assembly steps. This approach will reduce production costs and time and minimize waste and energy consumption, contributing to a lower environmental impact.

After an industrial case study is completed, final versions of the corrugated core sandwich panel samples can be produced for physical testing. These tests will validate the design, ensuring its reliability and consistency through quality control checks and identifying potential failure risks

References

[1] A. Krzyzak, M. Mazur, M. Gajewski, K. Drozd, A. Komorek and P. Przybyłek, "Sandwich structured composites for aeronautics:," *International journal of aerospace engineering ,* no. 7816912., 2016.

[2] J. Xiong, Y. Du, D. Mousanezhad, M. Eydani, "Sandwich structures with prismatic and foam cores: A review," *Advanced Engineering Materials ,* vol. 27, 2019.

[3] J. Galos, R. Das, M. P. Sutcliffe, A. P. Mouritz, "Review of balsa core sandwich composite structures," *Materials & Design,* p. 111013, 2022.

[4] K. Faidzi, S. Abdullah, M.F. Abdullah, A.H. Azman, "Review of current trends for metal-based sandwich panel: Failure mechniacm and their contribution factors," *Engineering failure analysis,* vol. 123, pp. 285-311, 2021.

[5] S. Mandegarian, M. Hojjati, H. Moghaddar, "Recycled PET foam core sandwich panels with reinforced hybrid composite facesheet: A sustainable approach for enhanced impact resistance," *Journal of sandwich structures & materials ,* 2024.

[6] V. A. Matsagar, "Comparative performance of composite sandwich panels and non-composite panels under blast loading," *Materials and Structures,* vol. 49, pp. 611-629, 2015.

[7] M. Alphonse, V.K. Bupesh Raja, V. Gopala Krishna, R. Sai Bupesh Raja "Mechanical behavior of sandwich structures with varying core material – A review," *materialtoday,* vol. 44, pp. 3751-3759, 2021.

[8] S. K. Sahu, P.S. Rama Sreekanth. S.V. Kota Reddy, "A Brief Review on Advanced Sandwich Structures with Customized Design Core and Composite Face Sheet," *polymers,* 2022.

[9] L. Ke, K. Liu, G. Wu, Z. Wang, P. Wang "Multi-Objective Optimization Design of Corrugated Steel Sandwich Panel for Impact Resistance," *metals,* vol. 11, no. 9, 2021.

[10] E. Elghandour, N. Elzayady, "Comparison between honeycomb and composite corrugated cores in sandwich panels under compression loading," *Sustainable Materials and Structural Systems ,* vol. 5, pp. 179-192, 2021.

[11] M.R.M. Rejab, N.Z.M. Zaid, N.A.N Mohamed, "Sandwich Structure Based On Corrugated-Core: A Review," in *ICMER*, 2016.

[12] W. He, J. Liu, D. Xie, B. Tao, "Experimental and numerical research on the low velocity impact behavior of hybrid corrugated core sandwich structures," *Composite Structures,* vol. 158, pp. 30-43, 2016.

[13] R. Rejab, W.J. Cantwell, "The mechanical behaviour of corrugated-core sandwich panels," *Composites Part B: Engineering ,* vol. 47, pp. 267-277, 2013.

[14] M. Jayakrishna, M. Vijay, B. Khan, "An Overview of Extensive Analysis of 3D Printing Applications in the Manufacturing Sector," *Journal of Engineering ,* vol. 19, pp. 1-23, 2023.

[15] K. M. S. Sastry, Sandwich Panel Systems: Design and Applications, Springer , 2017.

[16] A. Lamichhane, A. K. Vasudevan, M. Mohammadabadi, K. Ragon, J. Street, R.D. Seale, "From Crop Residue to Corrugated Core Sandwich Panels as a Building Material," *materials,* vol. 18, no. 1, 2024.

[17] T. Khan, V. Acar, M. R. Aydin, B. Hulagu, "A review on recent advances in sandwich structures based on polyurethane foam cores," *Polymer Composites ,* vol. 41, no. 6, pp. 2355-2400, 2020.

[18] K. A. Brekken, A. Reyes, M. Langseth, T. Berstad "Sandwich Panels with Polymeric Foam Cores Exposed to Blast Loading: An Experimental and Numerical Investigation," *applied aciences ,* vol. 10, no. 24, 2020.

[19] S. Mandegarian, M. Hojjati, H. Moghaddar, "Thermoplastic composite sandwich panels with recycled PET foam core: A manufacturing process assessment," *Journal of Thermoplastic Composite Materials ,* 2024.

[20] K. Yamada, Y. Shinohara, K. Ijima, K. Halada, "Recent Ecomaterial Developments and Environmental Achievements of Major Industries in Japan," *MATERIALS TRANSACTIONS,* vol. 48, no. 12, 2007.

[21] P. Benyathiar, P. Kumar, G. Carpenter, J. Brace, D. K. Mishra, "Polyethylene Terephthalate (PET) Bottle-to-Bottle Recycling for the Beverage Industry: A Review," *polymers,* vol. 14, no. 11, 2022.

[22] R. Chen, S. Deng, T. Cui, S. Duan, "Progress in recycling and reutilization of waste polyethylene terephthalate," *Progress in Rubber, Plastics and Recycling Technology,* vol. 40, no. 1, 2023.

[23] T. George, K. Sharp, V.S. Deshpande, H.N.G. Wadley, "Hybrid core carbon fiber composite sandwich panels: Fabrication and mechanical response," *Composite Structures,* vol. 108, no. 1, 2013.

[24] W. He, J. Liu, D. Xie, B. Tao, "Experimental and numerical research on the low velocity impact behavior of hybrid corrugated core sandwich structures," *composite structures,* vol. 158, pp. 30-43, 2016.

[25] S. M. Dolati Shokoofeh, "High velocity impact response of corrugated core composite sandwich structures," *Journal of Composite Materials ,* vol. 56, no. 16, pp. 2559-2571, 2022.

[26] P. Zhang, Y. Cheng, L. Jun, "Numerical analysis of dynamic response of corrugated core sandwich panels subjected to near-field air blast loading," *Shock and Vibration,* 2014.

[27] C. Thill, I.P. Bond, J. Etches, K. Potter, "Investigation of trapezoidal corrugated aramid/epoxy laminates under large tensile displacements transverse to the corrugation direction," *Composites: Part A,* vol. 41, pp. 168-176, 2010.

[28] J.S. Yang, J. Xiong, L. Ma, L.N. Feng, S.Y. Wang, L.Z. Wu, "Modal response of all-composite corrugated sandwich cylindrical shells," *Composites Science and Technology,* vol. 115, pp. 9-20, 2015.

[29] A. Vakilifard, H. Mazaherri, M. Shaban, "Bending behavior and geometrical optimization of five-layered corrugated sandwich panels with equal in-plane principal stiffness," *Journal of Composite Materials ,* vol. 56, no. 17, 2022.

[30] S. Sun, D. Liu, S. Yinglong, S. Feng, "Out-of-plane compression of a novel hybrid corrugated core sandwich panel," *Composite Structures,* vol. 272, 2021.

[31] A. Farrokhabadi, H. Madadi, S.A. Taghizadeh, H. Norouzi, "Experimental and numerical analysis of novel multi-layer sandwich panels under three point bending load," *Composite Structures,* vol. 250, 2020.

[32] H. Al-Rifaie, R. Studzinski, T. Gajewski, M. Malendosski, W. Sumelki, P. W. Sielicki, "A New Blast Absorbing Sandwich Panel with Unconnected Corrugated Layers—Numerical Study," *energies,* vol. 14, no. 1, 2021.

[33] S. Shi, Y. Chen, J. Liang, C. Dai, "Modeling the high temperature behavior of all composite, corrugated-core sandwich panels undergoing ablation," *Thin-Walled Structures,* 2021.

[34] F. Xia, T. Pang, G. Sun, D. Ruan, "Longitudinal bending of corrugated sandwich panels with cores of various shapes," *Thin-Walled Structures,* vol. 173, 2022.

[35] H. Abedzade Atar, M. Zarrebini, H. Hasani, Jalil Rezaeepazhand, "The effect of core geometry on flexural stiffness and transverse shear rigidity of weight-wise identical corrugated core sandwich panels reinforced with 3D flat spacer knitted fabric," *POLYMER COMPOSITES,* vol. 41, no. 9, pp. 3638-3648, 2020.

[36] S.V. Hoa, M. Abdali, A. Jasmin, D. Radeschi, V. Prats, H. Faour, "Development of a new flexible wing concept for Unmanned Aerial Vehicle using corrugated core made by 4D printing of composites," *Composite Strucutres ,* vol. 290, 2022.

[37] Y. Rong, J. Liu, W. He, W. Luo, "Effects of geometric configurations of corrugated cores on the local impact and planar compression of sandwich panels," *Composites Part B: Engineering ,* vol. 152, pp. 324-335, 2018.

[38] V. Acanfora, M. Zarrelli, A. Riccio, "Experimental and numerical assessment of the impact behaviour of a composite sandwich panel with a polymeric honeycomb core," *International Journal of Impact Engineering ,* vol. 171, 2023.

[39] F. Duddeck, C. W. Isaac, "Current trends in additively manufactured (3D printed) energy absorbing structures for crashworthiness application – a review," *Virtual and Physical Prototyping ,* vol. 17, no. 4, pp. 1058-1101, 2022.

[40] M. Kheradpisheh, M. Hojjati, "A novel compaction roller with variable pressure distribution and contact time for automated fiber placement: Experimental and numerical analysis," *Composites Part A: Applied Science and Manufacturing,* vol. 190, 2025.

[41] N. Iranmanesh, H. Yazdani Sarvestai, B. Ashrafi, M. Hojjati, "Beyond honeycombs: Core topology's role in 3D-printed sandwich panels," *materialstoday COMMUNICATIONS,* vol. 37, 2023.

[42] N. Zohdi, R. Yang, "Material Anisotropy in Additively Manufactured Polymers and Polymer Composites: A Review," *polymers,* vol. 13, no. 19, 2021.

[43] R. Williams, M. E. Bahadir, "Understanding the Anisotropic Characteristics of 3D Printed Parts," in *ASEE Gulf-Southwest Annual Conference*, 2022.

[44] N. Zohdi, P. Q. K. Nguyen, R. Yang, "Evaluation on Material Anisotropy of Acrylonitrile Butadiene Styrene Printed via Fused Deposition Modelling," *applied sciences,* vol. 14, no. 5, 2024.

[45] M. Oushti, B. Soufiane, B. El Haddadi, "Effect of Printing Parameters on the Mechanical Properties of Parts Fabricated with Open-Source 3D Printers in PLA by Fused Deposition Modeling," *Mechanics and Mechanical Engineering ,* vol. 22, no. 4, 2018.

[46] M. Khodaei, M. Haghighi-Yazdi, M. Safarabadi, M. A. Farzannia, "On the ballistic impact behavior of foam-filled honeycomb core/composite skin sandwich panels," *Journal of the Brazilian Society of Mechanical Science and Engineering,* vol. 45, 2023.

[47] V.A. Nagarajan, E. Dhanesh, K.P. Vinod Kumar, "Mechanical performance of stitched foam-filled honeycomb sandwich panels," *Proceedings of the Institution of Mechanical Engineers, Part C: Journal of Mechanical Engineering Science,* vol. 238, no. 19, 2024.

[48] R.S. Jayaram, V.A. Nagarjan, K.P. Vinod Kumar, "Compression and low velocity impact response of sandwich panels with polyester pin-reinforced foam filled honeycomb core," *Journal of Sandwich Structures & Materials ,* 2018.

[49] D. V. Marques, R. Barcelos, H.R.T. Silva, P. Egert, "Recycled polyethylene terephthalate-based boards for thermal-acoustic insulation," *Jouranl of cleaner Production ,* vol. 189, pp. 251-262, 2018.

[50] P. N. Ashtiani, "Moisture diffusion and its effect on performance of thermoplastic composite sandwich panels with recycled PET foam cores," Concordia University., Montreal, 2024.

[51] L. Doyle, I. Wedlich, "Moisture uptake and effects of hygrothermal exposure on closed-cell semicrystalline polyethylene terephthalate foam," *Polymer Degredation and Stability ,* vol. 202, 2022.

[52] M. Yazici, D. Bertin, J. Wright, A. Shukla, "Preferentially Filled Foam Core Corrugated Steel Sandwich Structures for Improved Blast Performance," *Journal of Applied Mechanics ,* vol. 82, no. 6, 2015.

[53] Y. Wang, Y. Guo, H. Wu, Q. Kan, H. Liu, J. Zhang, "Dynamic response of clamped sandwich beams with foam-filled sinusoidal corrugated core subjected to low-velocity impact," *Mechanics of Advanced Materials and Structures ,* 2024.

[54] Y. Cheng, T. Zhou, Y. Li, H. Wang, "Numerical investigation on the dynamic response of foam-filled corrugated core sandwich panels subjected to air blast loading," *Journal of Sandwich Structures and Materials ,* vol. 21, no. 3, pp. 838-864, 2019.

[55] H. Taghpoor, M. Sefidi, "Energy absorption of foam-filled corrugated core sandwich panels under quasi-static loading," *Journal of Materials: Design and Applications,* vol. 237, no. 1, 2022.

[56] S.A. Taghizadeh, A. Farrokhabadi, Gh. Liaghat, E. Pedram, H. Malekinejad, S. F. Mohammadi, H. Ahmadi, "Characterization of compressive behavior of PVC foam infill

composite sandwich panels with differnt corrugated core shapes," *Thin-Walled Structures ,* vol. 135, pp. 160-172, 2019.

[57] T. J. Lu. Y.S. Tian, "Optimal design of compression corrugated panels," *Thin-Walled Structures,* vol. 43, no. 3, pp. 477-498, 2005.

[58] C. Liang, M. Yang, P. Wu, "Optimum design of metallic corrugated core sandwich panels subjected to blast loads," *Ocean Engineering ,* vol. 28, no. 7, pp. 825-861, 2001.

[59] J. Zhang, P. Supernak, S. Mueller-Alander, C. H. Wang"Improving the bending strength and energy absorption of corrugated sandwich composite structure," *Materials & Design,* vol. 52, pp. 767-773, 2013.

[60] G. Akhmet, P. Hu, Y. Yu, W. Hou, "Analysis of the performance of adhesively bonded corrugated core sandwich structures using cohesive zone method," *Jouranal of Sandwich Structures & Materials,* vol. 22, no. 1, 2017.

[61] S. Pathirana, P. Qiao, "Local buckling analysis of periodic sinusoidal corrugated composite panels under uniaxial compression," *Composite Structures,* vol. 220, pp. 148-157, 2019.

[62] J. Edgar, S. Tint, "additive Manufacturing Technologies: 3D Printing, Rapid Prototyping, and Direct Digital Manufacturing" (2nd ed.), Springer, 2015.

[63] G. Morettini, L. Capponi, M. Palmieri, L. Landi, "Comprehensive characterization of mechanical and physical properties of PLA structures printed by FFF-3D-printing process in different directions," *Progress in Additive Manufacturing,* vol. 7, pp. 1111-1122, 2022.

[64] M. R. Khosravani, F. Berto, M. R. Ayatollahi, T. Reinicke, "Characterization of 3D-printed PLA parts with different raster orientations and printing speeds," *Scientific reports,* vol. 12, 2022.

[65] P. F. Mukoroh, F. Gouda, M. Skrifvars, and S. K. Ramamoorthy, “Influence of the manufacturing method (3D printing and injection molding) on water absorption and mechanical and thermal properties of polymer composites based on poly(lactic acid),” *Polymers*, vol. 16, no. 12, p. 1619, Jun. 2024

[66] L. Ranakoti, B. Gangil, S. K. Mishra, T. Singh, S. Sharma, R. A. Ilyas, and S. El-Khatib, “Critical review on polylactic acid: Properties, structure, processing, biocomposites, and nanocomposites,” *Materials*, vol. 15, no. 12, p. 4312, Jun. 2022.

[67] A. D638-22, "Standard Test Method for Tensile Properties of Plastics," ASTM International, West Conshohocken, 2022.

[68] A. A. Al-Tamimi, A. Pandzic, E. Kadric, "Investigation and Prediction of Tensile, Flexural, and Compressive Properties of Tough PLA Material Using Definitive Screening Design," *polymers ,* vol. 15, 2023.

[69] A. D695-23, "Standard Test Method for Compressive Properties of Rigid Plastics," ASTM International, 2023.

[70] ARMACELL, [Online]. Available: https://www.armacell.com/en-GB.

[71] Z. Zhang, C. Xin, C. Ma, W. Xu, "Morphology and Compressive Properties of Extruded Polyethylene Terephthalate Foam," *polymers ,* vol. 16, 2024.

[72] A. C365, "Standard Test Method for Flatwise Compressive Properties of Sandwich Core Materials," ASTM International, 2023.

[73] A. C393, "tandard Test Method for Flexural Properties of Sandwich Core Materials," ASTM International, 2023.

[74] M. Sefidi, H. Taghipoor, "Analysis of deformation and failure mechanism of sandwich beams with lattice core under three-point bending load," *Scientific Reports ,* vol. 14, 2024.

[75] E. Linul, L. Marsavina, Mechanical Characterization of Rigid PUR Foams Used for Wind Turbine Blades Construction, The world academic publishing co., 2013.

[76] S. Kazemahvazi, J. Kiele, B.P. Russell, V.S. Deshpande, "Impact proprties of corrugated composite sandwich cores," in *9th international conference on sandwich structures*, California, 2010.

[77] G. Bartolozzi, N. Baldanzini, M. Pierini, G. Zonfrillo, "Static and dynamic experimental validation of analytical homogenization models for corrugated core sandwich panels," *Composite Structures ,* vol. 125, pp. 343-353, 2015.